

ERG ANALYSIS REVEALS REDUCED FUNCTION IN ON-CENTER BIPOLAR  
CELLS OF GLUCOSE-TREATED ZEBRAFISH

By

Zaid Tanvir

Submitted to the

Faculty of the College of Arts and Sciences

of American University

in Partial Fulfillment of

the Requirements for the Degree

of Master of Science


In

Biology

Chair:

  
Victoria Connaughton, Ph.D.

  
Colin Saldanha, Ph.D.

  
Nancy Zeller, Ph.D.



Dean of the College of Arts and Sciences

April 29, 2013

Date

2013  
American University  
Washington, D.C. 20016

© COPYRIGHT

by

Zaid Tanvir

2013

ALL RIGHTS RESERVED

## DEDICATION

To my mother, who instilled in me the great value of continued education.

ERG ANALYSIS REVEALS REDUCED FUNCTION IN ON-CENTER BIPOLAR  
CELLS OF HYPERGLYCEMIC ZEBRAFISH

BY

Zaid Tanvir

ABSTRACT

Retinopathy is established as a consequence of diabetes mellitus in humans and has proven to lead to irreversible visual loss, often ending in blindness. Alterations in biochemical interactions in the retina due to chronic hyperglycemia can damage retinal vasculature leading to varying degrees of visual loss in diabetic individuals. This study proposes to further establish *Danio rerio* as an animal model for diabetic retinopathy. After inducing hyperglycemia in zebrafish through alternation between glucose-treated and normal water, retinal physiology was studied using ERGs to identify functional changes in the retinal tissues. Results revealed retinas exposed to glucose for 30 days had reduced b-wave activity in ERGs when compared to osmotic and water controls indicating reduced ON-center bipolar cell functionality. Reduced b-wave amplitudes were observed at peak absorption wavelengths for all four cone types. Reduced functionality in zebrafish retinas after glucose exposure supports their establishment as an animal model for diabetic retinopathy.

## ACKNOWLEDGMENTS

I would like to express my deep gratitude to my mentor Victoria Connaughton for her guidance, enthusiastic encouragement, and patience. I would also like to thank Ralph Nelson for his time and instruction. Last I would like to thank my friends and family for their endless support and cheer.

## TABLE OF CONTENTS

ABSTRACT .....	ii
ACKNOWLEDGMENTS .....	iii
LIST OF TABLES .....	vi
LIST OF FIGURES .....	vii
CHAPTER 1 INTRODUCTION .....	1
Vertebrate Retina .....	2
Diabetes Mellitus .....	7
Electroretinogram (ERG).....	13
Zebrafish .....	16
CHAPTER 2 EXPERIMENTAL DESIGN .....	20
Fish Maintenance .....	20
Hyperglycemic Induction.....	20
Preparation of Retinal Tissue and ERG Analysis .....	21
CHAPTER 3 RESULTS .....	24
Specimen Collection .....	24
Initial Data Analysis-Mean Responses .....	24
Subsequent Data Analysis of Individual Traces .....	27
Software-Generated Spectral Analysis .....	49
CHAPTER 4 DISCUSSION.....	52
Conclusion .....	56
Future Research .....	57

REFERENCES.....	64
-----------------	----

## LIST OF TABLES

### Tables

Table 1 Mean a- and b-wave Amplitudes for a 570nm Stimulus and Percent Change from Water Control for Mannitol and Glucose Treatment Groups, Blue Background ....	30
Table 2 Mean a- and b-wave Amplitudes for a 570nm Stimulus and Percent Change from Water Control for Mannitol and Glucose Treatment Groups, Red Background .....	32
Table 3 Mean a- and b-wave Amplitudes for a 490nm Stimulus and Percent Change from Water Control for Mannitol and Glucose Treatment Groups, Blue Background ....	34
Table 4 Mean a- and b-wave Amplitudes for a 490nm Stimulus and Percent Change from Water Control for Mannitol and Glucose Treatment Groups, Red Background .....	35
Table 5 Mean a- and b-wave Amplitudes for a 410nm Stimulus and Percent Change from Water Control for Mannitol and Glucose Treatment Groups, Blue Background ....	39
Table 6 Mean a- and b-wave Amplitudes for a 410nm Stimulus and Percent Change from Water Control for Mannitol and Glucose Treatment Groups, Red Background .....	39
Table 7 Mean a- and b-wave Amplitudes for a 370nm Stimulus and Percent Change from Water Control for Mannitol and Glucose Treatment Groups, Blue Background ....	42
Table 8 Mean a- and b-wave Amplitudes for a 370nm Stimulus and Percent Change from Water Control for Mannitol and Glucose Treatment Groups, Red Background .....	42
Table 9 Mean a- and b-wave Amplitudes for a 650nm Stimulus and Percent Change from Water Control for Mannitol and Glucose Treatment Groups, Blue Background ....	46
Table 10 Mean a- and b-wave Amplitudes for a 650nm Stimulus and Percent Change from Water Control for Mannitol and Glucose Treatment Groups, Red Background .....	46
Table 11 Mean Spectral Response Variable Comparison for all Three Treatment Groups, Blue Background .....	50
Table 12 Mean Spectral Response Variable Comparison for all Three Treatment Groups, Red Background.....	51



## LIST OF ILLUSTRATIONS

### Figures

Figure 1. Morphology of Vertebrate Retina showing the relation of different regions of the retina to each other (retinal pigmented epithelium, photoreceptor outer segments, ONL, OPL, INL, IPL, GCL, and Nerve Fiber layer) (Purves et al.,2008). .....	4
Figure 2. Zebrafish Eye (a) lens; (b) retina (c) cornea (d) choroid rete (e) nonkeratinizing epithelial cells (f) Bowman's membrane; (g) substantia propria (h) endothelium cells (i) pigment epithelium (j) cones and rods (k) bipolar cells (l) ganglion Cells (m) pre retinal vessels (Menke et al., 2011).....	7
Figure 3. Biological pathways activated by chronic exposure to hyperglycemia (Funatsu et al., 2006). .....	10
Figure 4. Progression of proliferative diabetic retinopathy is determined by the extent to which neovascularization occurs (Danis and Davis, 2008). .....	13
Figure 5. Basic wave form of an electroretinogram. a-wave, b-wave, d-wave, and oscillatory potentials are indicated (Nutzlich, 2004). .....	15
Figure 6. Various different possible alternations of the ERG from the normal; including hypernormal, delayed, reduced, extinguished, and negative orientations of the ERG (Nutzlich, 2004) .....	16
Figure 7. Zebrafish Gall Bladder and Pancreas. ....	17
Figure 9. Mean ERG Response to all wavelengths of Light and Levels of Neutral Density for all Glucose, Mannitol, and Water Treated Retinas, Blue Background.....	25
Figure 10 Mean ERG Response to all wavelengths of Light and Levels of Neutral Density for all Glucose, Mannitol, and Water Treated Retinas, Red Background.....	27
Figure 11 Mean ERG Responses to 570nm Stimulus for all Glucose, Mannitol, and Water Treated Retinas, ND 2.0, Blue Background.....	29
Figure 12 Mean ERG Responses to 570nm Stimulus for all Glucose, Mannitol, and Water Treated Retinas, ND 2.0, Red Background.....	31

Figure 13 Mean ERG Responses to 490nm Stimulus for all Glucose, Mannitol, and Water Treated Retinas, ND 2.0, Blue Background.....	33
Figure 14 Mean ERG Responses to 490nm Stimulus for all Glucose, Mannitol, and Water Treated Retinas, ND 2.0, Red Background.....	35
Figure 15 Mean ERG Responses to 410nm Stimulus for all Glucose, Mannitol, and Water Treated Retinas, ND 2.0, Blue Background.....	37
Figure 16 Mean ERG Responses to 410nm Stimulus for all Glucose, Mannitol, and Water Treated Retinas, ND 2.0, Red Background.....	38
Figure 17 Mean ERG Responses to 370nm Stimulus for all Glucose, Mannitol, and Water Treated Retinas, ND 2.0, Blue Background.....	40
Figure 18 Mean ERG Responses to 370nm Stimulus for all Glucose, Mannitol, and Water Treated Retinas, ND 2.0, Red Background.....	41
Figure 19 Mean ERG Responses to 650nm Stimulus for all Glucose, Mannitol, and Water Treated Retinas, ND 1.5, Blue Background.....	44
Figure 20 Mean ERG Responses to 650nm Stimulus for all Glucose, Mannitol, and Water Treated Retinas, ND 1.5, Red Background.....	45
Figure 21 Mean B-Wave Amplitude Comparison at Individual Wavelengths for All Treatment Groups, Blue Background.....	48
Figure 22 Mean B-Wave Amplitude Comparison at Individual Wavelengths for All Treatment Groups, Red Background.....	49

## CHAPTER 1

### INTRODUCTION

Retinopathy has been well established as a consequence of diabetes mellitus in humans and has proven to lead to irreversible visual loss, often ending in blindness (Deshpande, 2008). Alterations in biochemical interactions in the retina due to chronic hyperglycemia can damage retinal vasculature leading to varying degrees of visual loss in diabetic individuals (Deshpande, 2008). The purpose of this study is to further establish zebrafish (*Danio rerio*) as an animal model for diabetic retinopathy. Previous studies (Gleeson et al., 2006; Olsen et al, 2010) have established morphological changes in the retinal inner nuclear layer (INL) in zebrafish after 1 month of hyperglycemia. The homology of the zebrafish retina and human retina indicates that zebrafish will serve as an excellent animal model for the effects of diabetes on the retina.

After inducing hyperglycemia in zebrafish, the retinas can be studied using an electroretinogram (ERG) to determine if there are any functional changes to the retina. Previous literature has established that ERG recordings can be used to assess damage to the retina before clinical symptoms of retinopathy begin to appear (Ewing et al., 1998). Hyperglycemic conditions are known to alter the retinal vasculature leading to retinal cell death and decrements in functionality. The ERG recordings taken from hyperglycemia-induced fish are predicted to show degradation of retinal cell responses when compared to control fish.

## **Vertebrate Retina**

### **Anatomical Organization**

The retina consists of three nuclear layers that make up a peripheral part of the central nervous system as a vertebrate's primary means of photoreception. It is located at the back of the eye and is highly vascularized in humans. The outermost layer consists of rods and cones which are the photoreceptor cells. The middle layer consists of bipolar, horizontal, and amacrine cells and the inner layer consists of ganglion cells (Dowling, 1987). The axons of ganglion cells leave the eye through the optic disc and form the optic nerve (Purves et al., 2008).

In humans, the retinal vasculature nourishes the outer and inner layers of the retina, respectively (Cao et al., 2008). The choroidal vessels supply oxygen to the retina through the retinal pigmented epithelium and contain approximately 80% of the retina's blood supply. The remaining 20% enter through the central retinal artery, which emanates through the optic disc. In vascular retinas, these retinal vessels become intraretinal capillaries that nourish retinal cells via branches within the inner and outer plexiform layers (Cao et al., 2008). In avascular retinas, these vessels remain vitread to the ganglion cell layer and do not penetrate into the retina itself.

In order for the photoreceptors to be activated, light must pass through the cornea, aqueous humor, lens, and then the vitreous humor before it reaches the retina at the back of the eye. Since the morphology of the retina is inverted, light must pass through the layers of the retina and before being absorbed by photoreceptor cells or by the retinal pigment epithelium (Purves et al, 2008). The retinal pigment epithelium contains

melanin, which reduces the backscattering of light that enters the eye through the cornea (Sherwood et al., 2008).

Typically there are six different types of neurons in the retina (Dowling, 1987): rods, cones, bipolar cells, ganglion cells, horizontal cells, and amacrine cells. As light reaches the photopigment located in both types of photoreceptor cells, it alters the membrane potential of the cell causing changes in the release rate of the neurotransmitter glutamate. As seen in Figure 1, the cell bodies of photoreceptors make up the outer nuclear layer (ONL). They synapse with bipolar (and horizontal cells) in the outer plexiform layer (OPL). The bipolar cells, together with horizontal and amacrine cells, compose the inner nuclear layer (INL) and directly make contact with dendritic processes of ganglion cells in the inner plexiform layer (IPL). Ganglion cell axons converge at the optic disc to form the optic nerve which transmits signals to the thalamus and midbrain (Purves et al., 2008). Photoreceptor to bipolar to ganglion cell connections form the vertical transduction pathway through the retina.

The vertical transduction pathway is modified at two levels. Horizontal cell processes are located in the OPL and modulate lateral interactions between photoreceptor cells and bipolar cells as a means to enhance the retina's perception to contrast (Purves et al., 2008). Amacrine cell processes are located in the IPL and can perform various different functions, some of which are similar to those performed by horizontal cells. (Dowling, 1987).

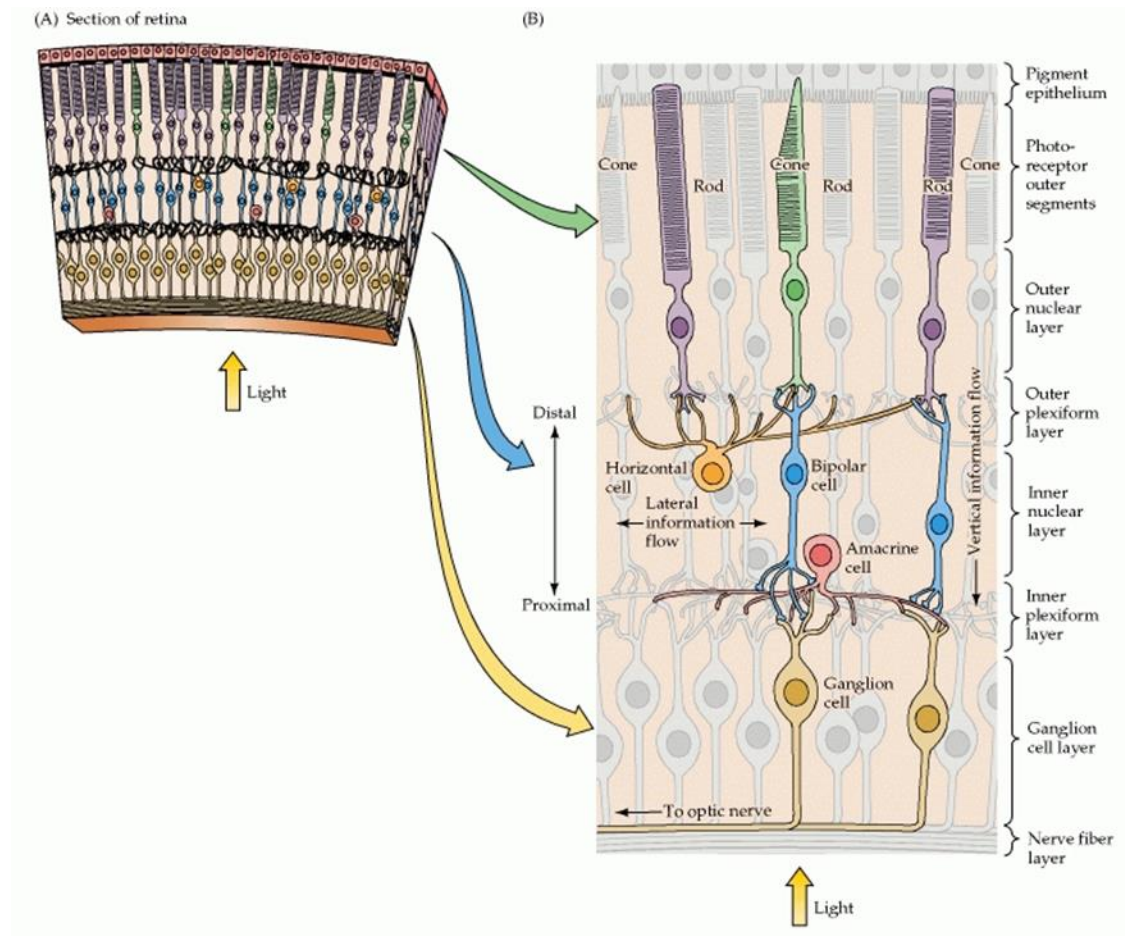


Figure 1. Morphology of Vertebrate Retina showing the relation of different regions of the retina to each other (retinal pigmented epithelium, photoreceptor outer segments, ONL, OPL, INL, IPL, GCL, and Nerve Fiber layer) (Purves et al., 2008).

## Phototransduction

Photoreceptor cells contain an outer segment that is surrounded by retinal pigmented epithelium (Purves et al., 2008). Membranous disks housed inside the outer segments contain a light-absorbing chemical named retinal, which is coupled with one of several different types of opsin proteins. It is the specific opsin protein that specializes a photoreceptor cell to a specific region of the electromagnetic spectrum. The opsin found in rods, rhodopsin, does not differentiate between different wavelengths within the visible

light spectrum, therefore rods do not perceive color. However there are different types of cone opsins. Colloquially, the varying cone types are called red, green, and blue cones, reflecting the different spectral sensitivities of the different cone opsins. These are also named long-wave (LW), middle-wave (MW), short-wave (SW) cones (Purves et al., 2008) in reference to the wavelength of light to which they are most sensitive. Zebrafish contain these cone types as well as UV cones (Robinson et al., 1995).

In darkness, the photoreceptor cells maintain a depolarized state and are constantly releasing the neurotransmitter glutamate into the OPL. As a photon of light is absorbed by the photopigments, cGMP levels in the outer segment decrease and a lack of cGMP-binding causes  $\text{Na}^+$  channels to close, reducing the influx of positive ions into the cell. Hyperpolarization results and glutamate release is reduced. On-center and off-center bipolar cells are differentially activated by these changes in glutamate release. On-center bipolar cells have G-protein coupled metabotropic receptors (mGluR6) that *hyperpolarize* the cell in response to glutamate binding. Off-center bipolar cells have ionotropic AMPA/kainate receptors that *depolarize* the cell when glutamate binds. On-center bipolar cells connect to on-center ganglions and together they detect increments of change in light whereas off-center bipolar cells connect to off-center ganglion cells and together they detect decrements of change in light. These two types of bipolar cells can be connected to the same cones in order to respond when lights are either on or off (Purves et al., 2008).

## **Zebrafish Retina**

The morphology of the zebrafish retina is comparable to the mammalian retina. As shown in Figure 2, the zebrafish retinal pigment epithelium is located at the back of the eye, distal to and around photoreceptor outer segments. Moving proximally is the ONL, OPL, horizontal cells, bipolar cells, amacrine cells, IPL, ganglion cell layer, and optic fiber layer (Yazulla et al., 2001). As in all other vertebrates, the IPL in zebrafish is broken into two layers, the distal sublamina a and the proximal sublamina b (Yazulla et al., 2001), which correspond to the connections between off-type and on-type cells, respectively. The zebrafish retina is also similar to that of humans in mural cell coating, endothelial cell junctions, and basement membrane composition (Alvarez, 2007).

The zebrafish retina is considered to be avascular (Chapman et al., 2009) because blood vessels do not penetrate into the retinal layers. Rather, the retina is nourished by a membranous layer of vasculature attached to the vitreous (Alvarez, 2007). The optic artery enters the vitreal space and remains vitread to the ganglion cell layer. Approximately 4 to 9 main vessels branch off the optic artery and pass through the optic disc. The vessels are then in direct contact with the ganglion cell layer (Alvarez, 2007, Cao, 2008), but do not penetrate into the retinal layers. Optic capillaries form a dense layer that constitutes two thirds the area of the optic disc (Cao, 2008).

Under normal conditions, many lower vertebrates, including the zebrafish, will experience retinomotor movements in their daily light/dark cycle. During light-adapted conditions, cones are shortened, rods elongate, and the pigment moves downward to cover the rod outer segments. In dark-adapted conditions, these movements are reversed:



cones lengthen, rods shorten, and the pigment moves upward. (Pierce and Besharse, 1985). These movements position cones so that they can absorb light in bright, daylight conditions (when rods are protected) and allow rods to be available to absorb light in dark conditions. Thus, this reorganization of retina tissue in response to light or dark conditions is presumed to be an adaptation to allow optimal light sensitivity in any lighted environment.

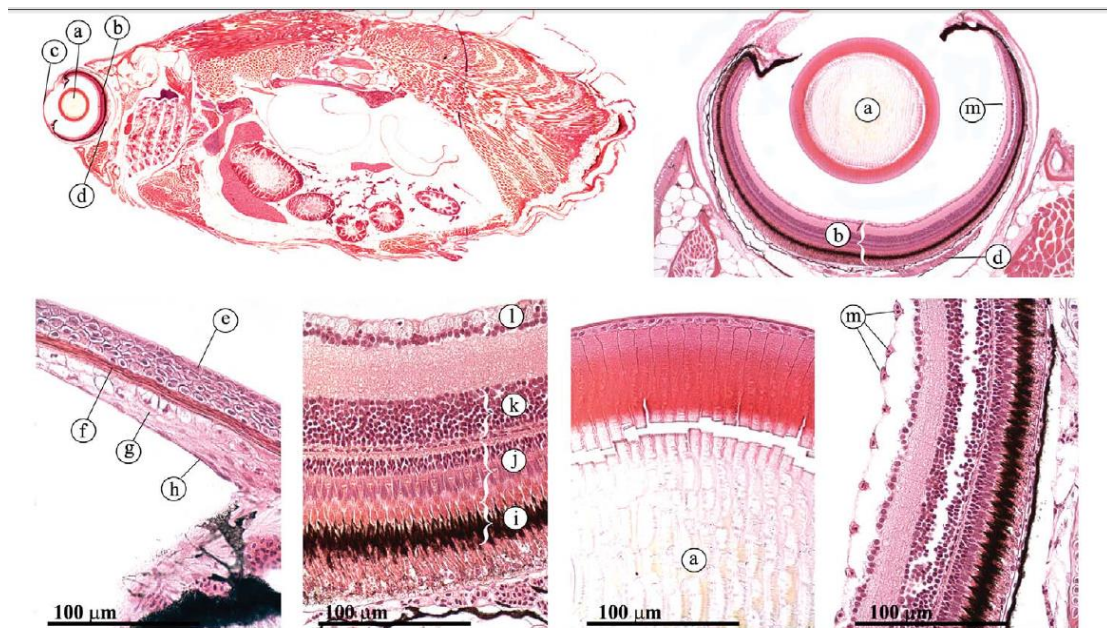


Figure 2. Zebrafish Eye (a) lens; (b) retina (c) cornea (d) choroid rete (e) nonkeratinizing epithelial cells (f) Bowman's membrane; (g) substantia propria (h) endothelium cells (i) pigment epithelium (j) cones and rods (k) bipolar cells (l) ganglion Cells (m) pre retinal vessels (Menke et al., 2011).

### Diabetes Mellitus

In 2005, an estimated 1.5 million new cases of diabetes were diagnosed and the number of individuals with diabetes is expected to triple by the year 2050 (Deshpande et al. 2008). Diabetes mellitus is characterized by various different symptoms that occur due to chronic high levels of glucose in the bloodstream (hyperglycemia). Normal blood

glucose values are maintained in a small range by endocrine regulation via  $\alpha$  and  $\beta$ -cells of the pancreas. During hypoglycemic conditions, such as skipping a meal,  $\alpha$ -cells of the pancreas release glucagon which signals liver and muscle cells to break down glycogen stores to increase the blood glucose level. Conversely, during hyperglycemic conditions, i.e., after consumption of a meal,  $\beta$ -cells of the pancreas release insulin to signal the body's tissues to upregulate glucose-transport across cell membranes (Deshpande et al. 2008), thereby reducing blood glucose levels.

Type I diabetes is a condition where pancreatic  $\beta$ -cells are destroyed by autoimmune responses from the body, thus leaving the body without a source of insulin. Type I is typically diagnosed during childhood and individuals with this form of the disease must take insulin injections to compensate for their inability to produce insulin. Type II diabetes is a condition where pancreatic  $\beta$ -cell function is normal; however, the body's tissues are insensitive to insulin signaling. Diagnosis of Type II typically occurs when individuals are older (adult-onset diabetes). Treatment in these individuals typically includes consistent monitoring of glucose levels and subsequent insulin injection in periods of hyperglycemia. Additionally, strict changes in diet are also encouraged to prevent chronic hyperglycemia from occurring. Gestational diabetes is similar to type 2 in that it is a form of insulin intolerance that affects women during their pregnancy (Deshpande et al. 2008).

Complications associated with diabetes are severe and can lead to either microvascular or macrovascular complications. Complications typically arise in individuals that have had diabetes for a prolonged period of time ( $>15$  years) (Meyerle et

al, 2008). Microvascular complications include nervous system damage (neuropathy), renal system damage (nephropathy), and retinal damage (retinopathy). Macrovascular complications include cardiovascular disease, stroke, and peripheral vascular disease (Meyerle et al., 2008).

### **Diabetic Retinopathy**

One complication of diabetes is a loss of visual function. This complication – diabetic retinopathy – is observed in individuals with diabetes for greater than 15 years and is clinically characterized and diagnosed by a change in retinal vasculature.

Since photoreception is an energy-expensive process, it requires the retina to be highly vascularized in order to meet its metabolic needs. Chronic hyperglycemic conditions associated with diabetes mellitus can cause microvascular degeneration in the retina. This includes retinal capillary microaneurysms, inflammation, vascular occlusion, increased vascular permeability, and eventual capillary closure or macular edema in retinal vasculature (Meyerle et al, 2008). These are all possible consequences of hyperglycemia that categorize the first stage of retinopathy - Non-Proliferative Diabetic Retinopathy (NPDR). The disease can progress further into Proliferative Diabetic Retinopathy (PDR) should the retina begin to develop neovascular tissue which can lead to tractional retinal detachment and vitreous hemorrhage ultimately ending in complete visual loss (Stitt, 2008).

Diabetic retinopathy is the most common microvascular complication from diabetes. It is a disease linked with degradation of retinal microvasculature due to glucose toxicity. Studies (as reviewed in Lorenzi et al., 2008) have shown that there are several

pathologies as to how hyperglycemia can be toxic to microvasculature; chronic polyol pathway activation, AGE production, electron transport chain disruption, and effects of osmotic stress. These mechanisms are laid out in the flow chart in Figure 3.

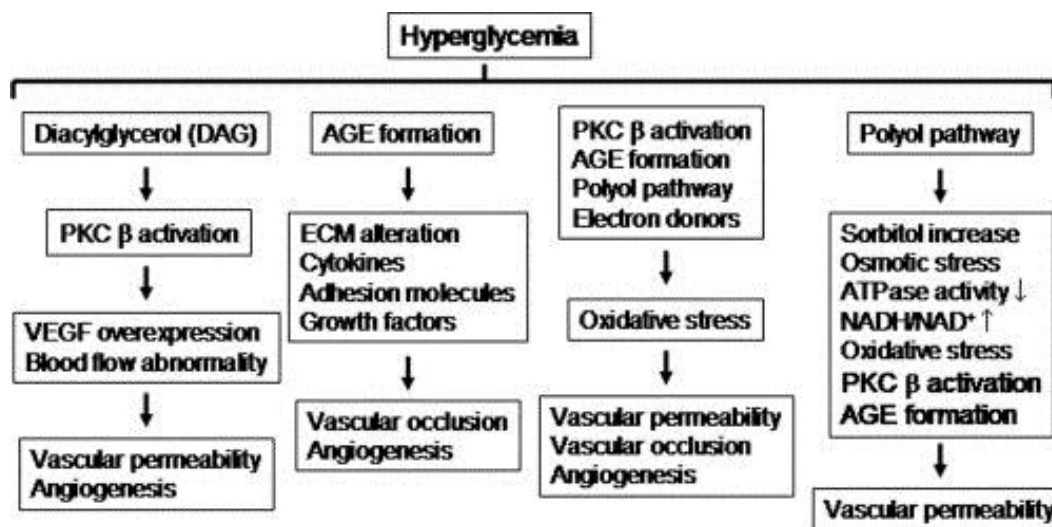


Figure 3. Biological pathways activated by chronic exposure to hyperglycemia (Funatsu et al., 2006).

The polyol pathway involves two enzymes: aldose reductase (AR) and soribitol dehydrogenase (SDH). The pathway converts glucose to sorbitol with the hydrolysis of NADPH to  $\text{NADP}^+$  by AR and sorbitol to fructose with  $\text{NAD}^+$  conversion to NADH by SDH. Chronic polyol pathway activation is due to high levels of glucose in the cytoplasm of the cell (a result of hyperglycemic conditions) which drives the reaction forward (Lorenzi et al., 2008).

Sorbitol is an alcohol that does not readily diffuse out of the cell membrane. Accumulation of sorbitol causes increases in osmotic pressure to the cell. Additionally, chronic activation of the polyol pathway causes oxidative stress due to competition for NADPH. NADPH is a cofactor involved with glutathione reductase which contributes to

maintaining low levels of oxidized glutathione. Similarly, in the second step of the reaction, creation of excessive amounts of NADH serves as a substrate for NADH oxidase to create superoxide (Lorenzi et al., 2008). Thus there is a net decrease in oxidant defense and a net increase in oxidant production in affected cells. The osmotic and oxidative pressures put onto the retinal capillary cells ultimately lead to apoptosis and the release of pro-inflammatory factors (Lorenzi et al., 2008).

Accordingly, the increase of glucose and fructose in the cell leads to an intracellular generation of advanced glycation endproducts (AGE). AGEs are produced from the nonenzymatic glycation reactions that occur when reducing sugars are present in excess in a cell. They combine with free amino groups, proteins, lipids, and DNA. The rate of formation of AGEs is irreversible and significantly higher in cells exposed to hyperglycemic conditions. The toxic effect of AGEs on the retinal microvasculature is through its promotion of oxidative stress and inhibition of superoxide dismutase activity (Stitt, 2008).

Hyperglycemia also can disrupt the normal functioning of the electron transport chain (ETC) in the mitochondria. Excess glucose in the cell will increase the number of electron donors such as NADH and  $\text{FADH}_2$  from the citric acid cycle. The membrane potential of the cristae in the mitochondrion subsequently increases due to the presence of these electron donors. This can lead to electron leakage from the ETC which can allow for superoxide to be produced in large quantities (Caldwell, 2008). The increasing oxidative stress on the affected cells can lead to apoptosis.

Hyperglycemia profoundly affects pericytes in the retinal vasculature. Pericytes are located in the capillary basement membrane (Pfister et al., 2008) and have many tight

junctions that function to strengthen the capillary walls. Pericyte-covered endothelial cells serve as a barrier to reduce extra fluid deposition (Meyler, 2008). The retina has one of the highest ratios of pericytes to endothelial cell number in the body (1:1). The high number of pericytes in the retinal microvasculature is thought to be due to its role in maintaining the blood-retinal barrier (Pfister et al., 2008). Pericytes are among the most likely cells to be affected by oxidative stress caused by hyperglycemia, which is reflected in the fact that pericyte loss is among the earliest signs of diabetic retinopathy.

The pathophysiology of NPDR begins with the loss of pericytes, as microaneurysm formation after pericyte loss is among the first visible signs (Meyerle et al. 2008). Morphologically, microaneurysms are overgrowths of the capillary cell wall, possibly due to endothelial cell proliferation after pericyte loss (Pfister et al., 2008). As NPDR progresses, there are increasing numbers of microaneurysms in the retina. Capillary closure ensues which leads to acellular capillaries and intraretinal hemorrhages.

Increased vascular permeability occurs due to both pericyte loss and hypoxia-induced release of vascular endothelial growth factor (VEGF). VEGF functions to promote the growth of new capillaries by first changing the conformation of tight junctions between vascular endothelial cells (Meyerle et al., 2008). As vascular permeability increases, more severe symptoms such as macular edema, or retinal thickening due to accumulated fluid, can occur. Though macular edema can occur without visual loss, chronic increases in vascular permeability can induce macular edema, causing permanent visual loss due to disruptions in retinal morphology (Meyerle et al., 2008).

As exposure to chronic hyperglycemia continues, the resulting chronic ischemia in the retina, due to non-perfusion in the vasculature, eventually leads to neovascularization, a hallmark of proliferative diabetic retinopathy (PDR). PDR usually develops in eyes experiencing severe NPDR (Danis and Davis, 2008). Neovascularization occurs in response to hypoxia. VEGF is released to promote new capillary cell growth which can be seen in Figure 4. However, after the new vascular tissues enlarge, they undergo a period of regression. The cycle of constant angiogenesis and regression of tissue, ultimately leads to tractional retinal detachment and vitreous hemorrhaging resulting in permanent visual loss. (Danis and Davis, 2008).

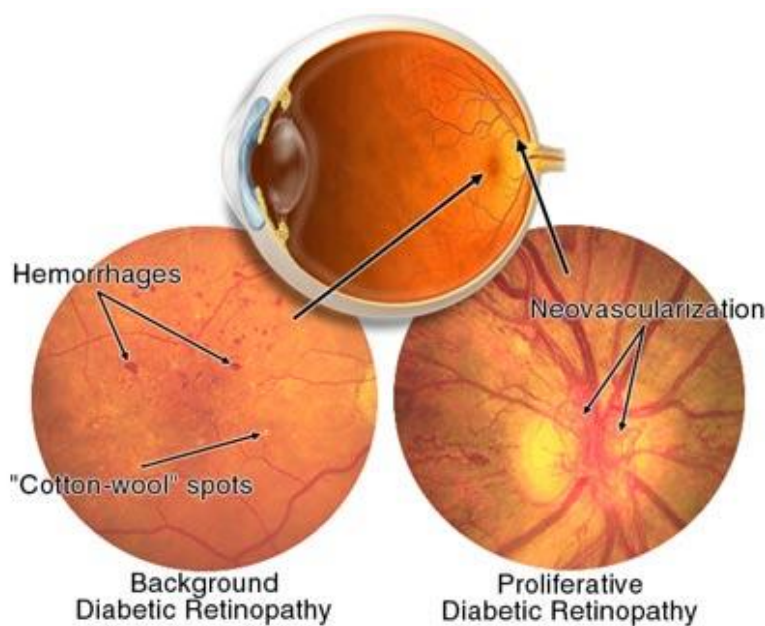


Figure 4. Progression of proliferative diabetic retinopathy is determined by the extent to which neovascularization occurs (Danis and Davis, 2008).

### **Electroretinogram (ERG)**

Electroretinograms (ERGs) have been used for decades as a means to evaluate the human retina for pathophysiological damage to functioning retinal tissue (Tzekov &

Arden, 1999). Using flashes of light, patterned stimulation, focused, or multifocused ERG analysis provides information attributed to the various layers of tissue in the retina and their specific functioning (Tzekov & Arden, 1999). The various forms of ERG reflect methods to determine functionality of the different retinal cell types involved in the optic pathway (Phipps et al., 2006). Cellular activity among rods, cones, ganglion cells, bipolar cells and other retinal cells involved in phototransduction can be specifically analyzed via the various methods (Phipps et al., 2006).

ERGs are measured by placing an electrode on the cornea and measuring the retina's response to a stimulating light. The resulting waveform includes various components, each attributed to a different type of retinal cell. a-wave, b-wave, and oscillatory potentials (OPs) are among the most commonly analyzed measures of ERG responses (Figure 5) and are used to assess retinal damage in individuals suffering from NPDR (Tzekov & Arden, 1999). a-waves represent the activity of photoreceptors. b-waves reflect the response of ON-type bipolar cells and/or Muller glial cells. d-wave responses are generated by OFF-bipolar cells and oscillatory potentials are due to amacrine cells. Oscillatory Potentials are wavelets that are superimposed onto the b-wave ERG on the ascending limb (Tzekov & Arden, 1999).



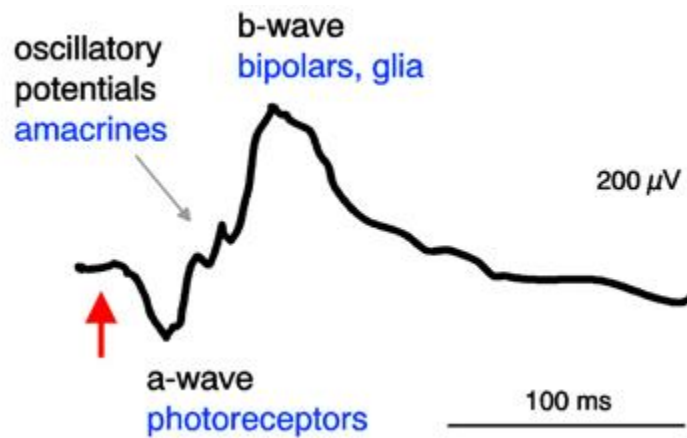


Figure 5. Basic wave form of an electroretinogram. a-wave, b-wave, d-wave, and oscillatory potentials are indicated (Nutzlich, 2004).

Changes in ERG waveforms can be varied (Figure 6). There has been sufficient evidence to show that changes in the ERG occur in individuals suffering from diabetes before the development of retinopathy (Ewing et al., 2009). Irregular ERG recordings, specifically in changes in OP amplitude, are reported in diabetic patients with no other evidence of retinopathy (i.e., no vascular changes are evident) when compared to control subjects (Ewing et al., 2009). Other studies have noted irregular ERG recordings such as reduced b-wave amplitudes in individuals with diabetic retinopathy (Papakostopoulos, 1996). Additionally, the patterned electroretinogram (PERG) is one type of ERG recording that has been able to show when there are early detectable pathophysiological signs of the development of NPDR (Ewing et al., 2009).

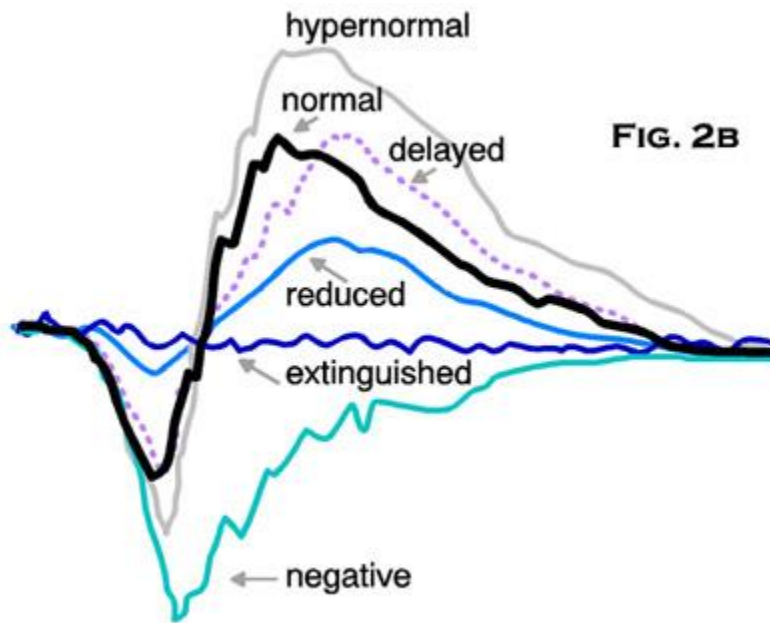


Figure 6. Various different possible alternations of the ERG from the normal; including hypernormal, delayed, reduced, extinguished, and negative orientations of the ERG (Nutzlich, 2004)

### Zebrafish

The zebrafish (*Dario rerio*) provides an excellent resource for testing the effects of hyperglycemia on the vertebrate retina. Previous studies (Gleeson et al., 2006, Olsen et al., 2010) have established the negative effects of hyperglycemia on the zebrafish retina including changes in INL and IPL thickness after induction of hyperglycemia.

Additionally, retinal cell organization in the zebrafish is similar to that of humans (Menke et al., 2011). Placement of the retinal pigment epithelium, external nuclear layer, bipolar and ganglion cell layers, and arrangement of ganglion axons in the optic nerve is also similar to the mammalian retina (Yazulla, 2001).

Though the exocrine pancreatic tissues of the zebrafish are scattered throughout the intestinal tract (Figure 7), the endocrine pancreatic tissues are very similar to mammals. The  $\alpha$ -cells produce glucagon-like protein and  $\beta$ -cells produce insulin (Menke

et al., 2011). Previous animal model studies have induced hyperglycemic conditions in the retina by the use of streptozotocin to knock out pancreatic  $\beta$ -cell production of insulin (Szkudelski, 2000). However, zebrafish have demonstrated an extraordinary ability to regenerate pancreatic  $\beta$ -cells (Pisharath et al., 2006, Moss et al., 2008) and thus the one-time use of streptozotocin would be insufficient in properly inducing hyperglycemia in the experimental fish. A study conducted by Olsen et al. (2010) showed that repeated injection of streptozotocin can continuously knock out  $\beta$ -cell function (2010). While this does seem to be an effective method for inducing hyperglycemia in zebrafish, studies have shown that streptozotocin is a carcinogen and can interfere with the zebrafish in ways other than destruction of  $\beta$ -cells (Bolzan and Bianchi, 2002).

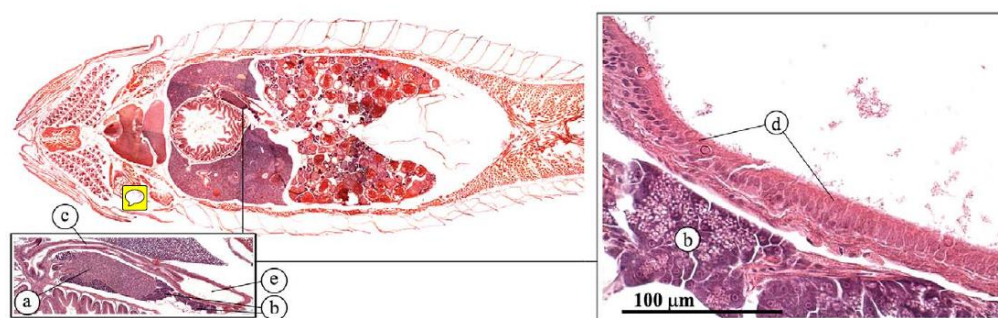


Figure 7. Zebrafish Gall Bladder and Pancreas. (a) Endocrine pancreas (Brockman Body); (b) exocrine pancreas; (c) common bile duct; (d) transitional gall bladder epithelium; (e) gall bladder (Menke et al., 2011).

Many studies examining diabetic retinopathy have focused on mammalian models such as primates, dogs, rats, mice, and other rodents (Meyerle et al., 2008). Of those studied, most animal models have developed at the very least the early stages of retinopathy. No known animal model will provide an exact replica of the pathology occurring in human diabetic retinopathy; however, there is great value in researching

models that may develop the early stages of retinopathy from the induction of hyperglycemia. Furthermore, animal models such as primates, dogs, and cats can take years to collect sufficient data (Meyerle et al., 2008). As an alternative, zebrafish are a significantly faster animal model of disease progression considering their short lifespan, small retinal size, and that hyperglycemia-induced changes are observed after 1 month of treatment. Abnormalities in morphology of zebrafish retina have already been established by induction of hyperglycemic conditions (Gleeson et. al, 2006).

In order to firmly establish zebrafish as a model for diabetic retinopathy in humans, it is important to determine if there are functional changes in the retina that correspond with documented anatomical changes. To determine if there are functional changes, ERGs can be performed following prolonged (1 month) hyperglycemic exposure. The speed at which zebrafish are able to reproduce and mature would not only accelerate the rate at which researchers could understand the mechanisms behind NPDR and PDR pathophysiology, but possibly also allow them to find ways to prevent early stages in diabetic individuals.

The purpose of this study is to examine physiological changes in the hyperglycemic zebrafish retina using ERG analysis to determine if functional changes reported in mammals, including humans, also occur in zebrafish. After a hyperglycemic treatment for 30 days, retinal physiology was examined. Our hypothesis is that retinal cells in hyperglycemic fish will show reduced functionality when compared to control fish, supporting anatomical findings. We expect to compare a-wave and b-wave forms between treatment groups, looking at changes in response amplitudes and timing of onset of each response. By focusing on retinal responses to individual wavelength stimuli, we

can determine if there is a loss of function of photoreceptors at specific wavelengths, suggesting which cone photoreceptor types may be compromised in hyperglycemic conditions.

## CHAPTER 2

### EXPERIMENTAL DESIGN

#### **Fish Maintenance**

Zebrafish adults were purchased from a vendor or bred from the in-house zebrafish colony and housed at American University's Hurst Building, Room 4, in an aquatic habitat. The fish were acclimated for at least one week to standard laboratory conditions of 28°C and a photoperiod of 14 hours of light and 10 hours of darkness prior to experiments. The fish were fed a diet of TetraMin flakes + zebrafish crumble diet daily until the beginning of the experiments. 12 fish were used in the first round of experiments that began in July of 2012. An additional 12 fish were used in the second round of experiments that began in October of 2012. The last 12 fish were used in the third and final round of experiments which began in January of 2013.

#### **Hyperglycemic Induction**

Hyperglycemia was induced in zebrafish by exposing the fish to alternating conditions of 2% glucose/0% glucose every 24 hours. Osmotic control animals were exposed to 2% mannitol/0% mannitol every 24 hours and the water control animals were exposed to 0% glucose/0% glucose every 24 hours. All water used in the experiments was identical except for the addition of glucose or mannitol to their respective tanks. All

fish were fed Tetramin flakes every other day starting on Day 2. Temperature, pH, water quality, and general fish behavior was recorded each day. Due to the time-intensive aspect of ERG analysis, the experimental groups were separated into three different trials (1) glucose treated group with a water control group, (2) glucose treated group with a mannitol (osmotic control) control group, and (3) mannitol control group with a water control group. Each round of exposure (trial) was conducted for at least 28 days before ERG analysis.

Starting on Day 28, two fish were prepared for ERG analysis. On each subsequent day, 2 fish were removed for physiological examination until all fish were examined. Alterations between the two solutions continued for all remaining fish until all fish had been analyzed. Fish were transported in 1L containers with 28°C Deer Park water to the NIH for analysis.

### **Preparation of Retinal Tissue and ERG Analysis**

Fish were sacrificed by decapitation. Each eye was removed from the fish after hemisection of the brain through a sagittal incision. Using forceps and iris scissors, an eye cup was made from each eye. The cornea, iris, and lens were surgically removed from the eye leaving the vitreous humor and the retina exposed. Eyecups were placed in oxygenated MEM solution in a dark room to recover. Eyecups were then sealed in a Faraday cage, housing the ERG electrode, grounding electrode, MEM perfusion tube, background light source, and stimulating light source. The eyecups were perfused with oxygenated MEM containing 1% CNQX. As an AMPA/Kainate receptor antagonist, CNQX functioned to inhibit all retinal synaptic signaling except between photoreceptor

and on-center bipolar cells. This allowed us to isolate the presynaptic a-wave and the postsynaptic b-wave of the ERG for analysis. The perfusion tube was placed inside the eyecup into the vitreous humor with a perfusion rate of 0.3mL per minute. The grounding electrode was placed close to the eyecup, but was covered to prevent any possible interference with the ERG electrode, which was also inserted into the vitreous humor.

Once each eyecup was in place and being perfused, a background light lit the stage to prevent the retina from undergoing dark adaption. Each protocol exposed the eye cup to 10 different wavelengths of light for 2 seconds each and recorded all evoked electrical responses. Wavelengths used ranged from 650nm (red light) to 370 (UV light). For each wavelength of light, the light intensity (defined by neutral density of the light stimulus) was increased 7 times before moving to the next wavelength. The protocol was run on each eyecup 4 times, twice with a blue background (wavelength of 418nm) and twice with a red background (wavelength of 627nm) to prevent dark-adaption. The change in background light color was performed to ensure that it was not impacting ERG results due to saturation of one cone type over another.

Electrode input in millivolts per half millisecond was recorded in Clampex software for each of the different wavelengths and dimness levels. Every protocol exposed the retina to each of the following wavelengths in order: 650nm, 570nm, 490nm, 410nm, 330nm, 650nm, 610nm, 530nm, 450nm, and 370nm. At each wavelength of light, brightness was changed by adding neutral density filters into the light path. Brightness values used ranged from 5.0 to 0.0 ND, with 5.0 being the dimmest and 0.0 being the brightest.



Clampex files were exported and analyzed using Origin 8.5 software. Origin files separated the data in the Clampex files into columns of information for each response recorded from the electrode. Origin 8.5 software also generated mean response plots for all wavelengths and all neutral densities for the different stimulating protocol. Each column represented the millivolt values (recorded from the electrode in the eyecup) per half millisecond interval in response to the light stimulus. The spectral sensitivity of each of the four cone types was modeled as in (Connaughton and Nelson, 2010; Nelson and Singla, 2009). The spectral sensitivity for red, green, blue, and UV cones were defined by the variables  $V_r$ ,  $V_g$ ,  $V_b$ , and  $V_u$ , respectively. Data was imported into SPSS software for statistical analysis and plotting of mean ERGs for comparison.

### **Statistics**

A comparison of means was conducted for the maximum b-wave amplitudes for the nine glucose group fish were compared to those of the nine control group fish using a t-test. The analysis was done using Microsoft Excel software.

## CHAPTER 3

### RESULTS

#### **Specimen Collection**

Fish were maintained in alternating glucose (2%), mannitol (2%), or control/water (0%) conditions for 28-33 days. To make sure all fish could be physiologically analyzed after approximately 1 month of treatment, fish were treated in 3 separate trials. Trial 1 included glucose- and water-treated (control); trial 2 tested glucose- and mannitol-treated fish; and trial 3 included mannitol- and water-treated fish. Overall survival was good in all treatments, with physiological recordings made from 33 of the 36 fish. Of the 66 intact eyes available, ERG analysis was performed successfully on 44 eyes from a total of 27 fish (15 eyes from 9 glucose fish, 15 eyes from 9 mannitol fish, 14 eyes from 9 control fish).

#### **Initial Data Analysis- Mean Responses**

To determine if there were any general trends within the data, mean ERG responses elicited by all stimulating wavelengths on both the red and blue adapting backgrounds were plotted for all three treatment groups. To avoid pseudoreplication, when both eyes from the same fish were physiologically examined, the eye selected for analysis was randomly chosen. As a result, within each treatment group, a total of 9 eyes

were analyzed, each from a separate zebrafish. As seen in Figure 9, there is no obvious discrepancy in overall waveform between the three treatment groups when the stimuli were presented with a blue adapting background. In each group there is a negative-going a-wave at light onset followed by a large, positive b-wave. However, in regard to amplitude, mannitol and water treatment groups have an equal response, whereas the glucose-treated retinas have reduced b-wave. a-wave response amplitudes appear similar among all three groups.

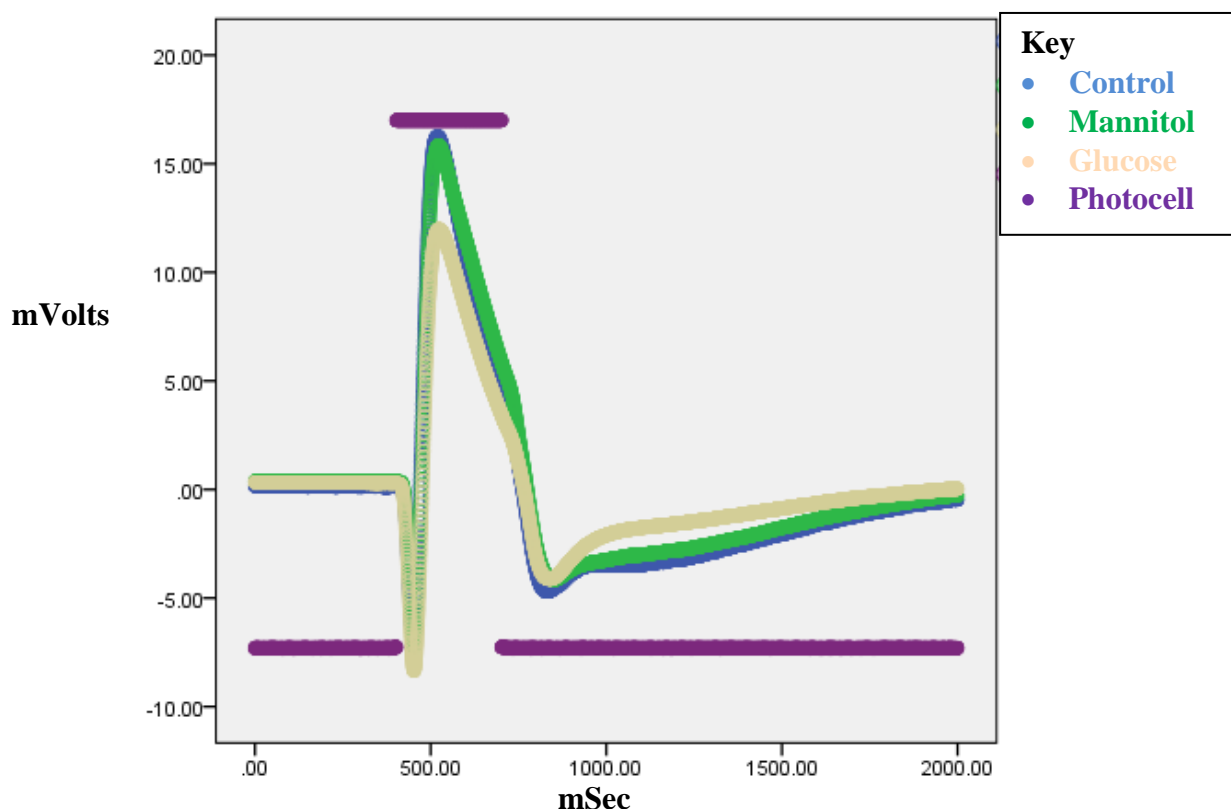


Figure 9. Mean ERG Responses to all Wavelengths of Light and Levels of Neutral Density for all Glucose, Mannitol, and Water Treated Retinas, Blue Background. For each treatment group, the mean ERG response for all wavelengths and neutral density (ND) for each individual protocol performed with a blue (418nm) background stimulus were averaged together to produce a comparison of overall mean ERG responses. Each treatment group contains 9 retinas from separate fish. The mean ERG response from glucose-treated, mannitol-treated, and water control are seen in grey, green, and blue, respectively. The light stimulus activation is shown in purple. The figure shows a

reduction in amplitude of the b-wave in glucose-treated retinal response . Mean mannitol-treated retinal response seems to be equal to that of the water-control retinal response.

Similar traces were also plotted for the red-adapting background (Figure 10), with the same general waveforms recorded for the three treatment groups: a negative-going a-wave and a positive b-wave. However, as observed for recordings elicited with a blue adapting background, the responses of glucose treated retinas with a red adapting background had a reduced b-wave amplitude when compared to the other two treatment groups. One difference between responses with the blue adapting background and responses with the red adapting background was that the mean response of the mannitol-treated eyes had a slightly lower b-wave amplitude than the water control group when the red adapting background was used. a-wave responses appeared similar among all three groups, regardless of adapting background.

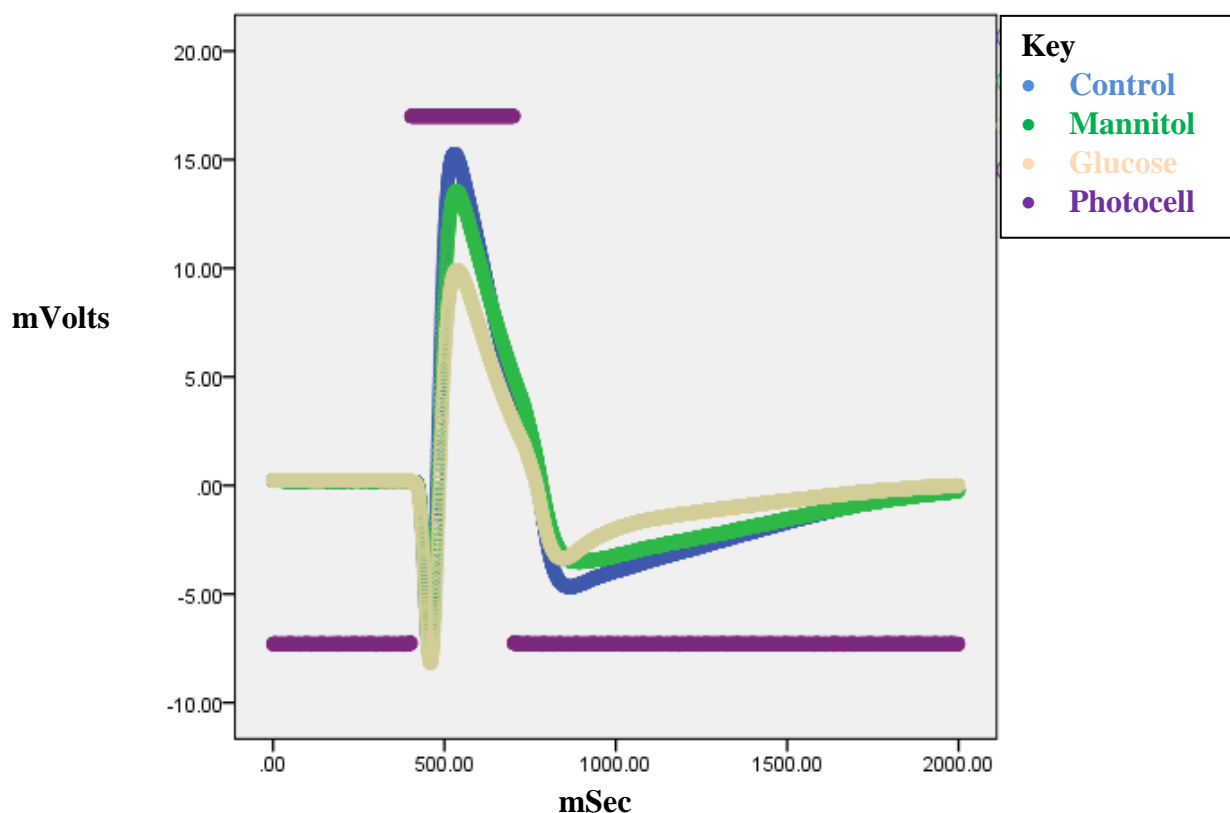


Figure 10. Mean ERG Responses to all Wavelengths of Light and Levels of Neutral Density for all Glucose, Mannitol, and Water Treated Retinas, Red Background. For each treatment group, the mean ERG response for all wavelengths and neutral density (ND) for each individual protocol performed with a red (627nm) background stimulus were averaged together to produce a comparison of overall mean ERG responses. Each treatment group contains 9 retinas from separate fish. The mean ERG response from glucose-treated, mannitol-treated, and water control are seen in grey, green, and blue, respectively. The light stimulus activation is shown in purple. The figure shows a decrease in amplitude of the b-wave in glucose-treated retinal responses. Mean mannitol-treated retinal response seems to be close, but not equal to that of the water-control retinal response.

### Subsequent Data Analysis of Individual Traces

To determine if the differences in retinal function seen in the mean ERG response plots were due to changes in individual cones, the mean ERG responses elicited by individual stimulating wavelengths were plotted using the methods described above. Again, to avoid pseudoreplication, when ERGs were recorded from both eyes from the same fish, the eye selected for analysis was randomly chosen. Figures were produced by

creating mean ERG response plots for each group at the following wavelengths: 650nm (1.5 ND), 570nm (2.0 ND), 490nm (2.0 ND), 410nm (2.0 ND), and 370nm (2.0 ND). For each wavelength, two mean ERG response plots were generated, one for each adapting color background. A neutral density (ND) of 2.0 was selected as the brightness level for analysis for most wavelengths, as this was the brightest stimulus that all retinas were exposed to and thus was the brightest stimulus intensity for which a mean response could be calculated.

The mean ERG response to the 570nm stimulus – corresponding to the  $\lambda_{\text{max}}$  for the red cone opsin - for each treatment group on a blue adapting background (Figure 11) shows the overall waveform for all treatment groups is similar in response. There is no delayed onset of either the a-wave or the b-wave for any treatment group. However, there is a discrepancy among b-wave amplitudes, which are reduced by 43.3% in responses from the glucose-treated retinas (Table 1), compared to the mannitol and water control groups. The mean b-wave response amplitude for the mannitol group is slightly larger than that of the water control group by 13.5%.

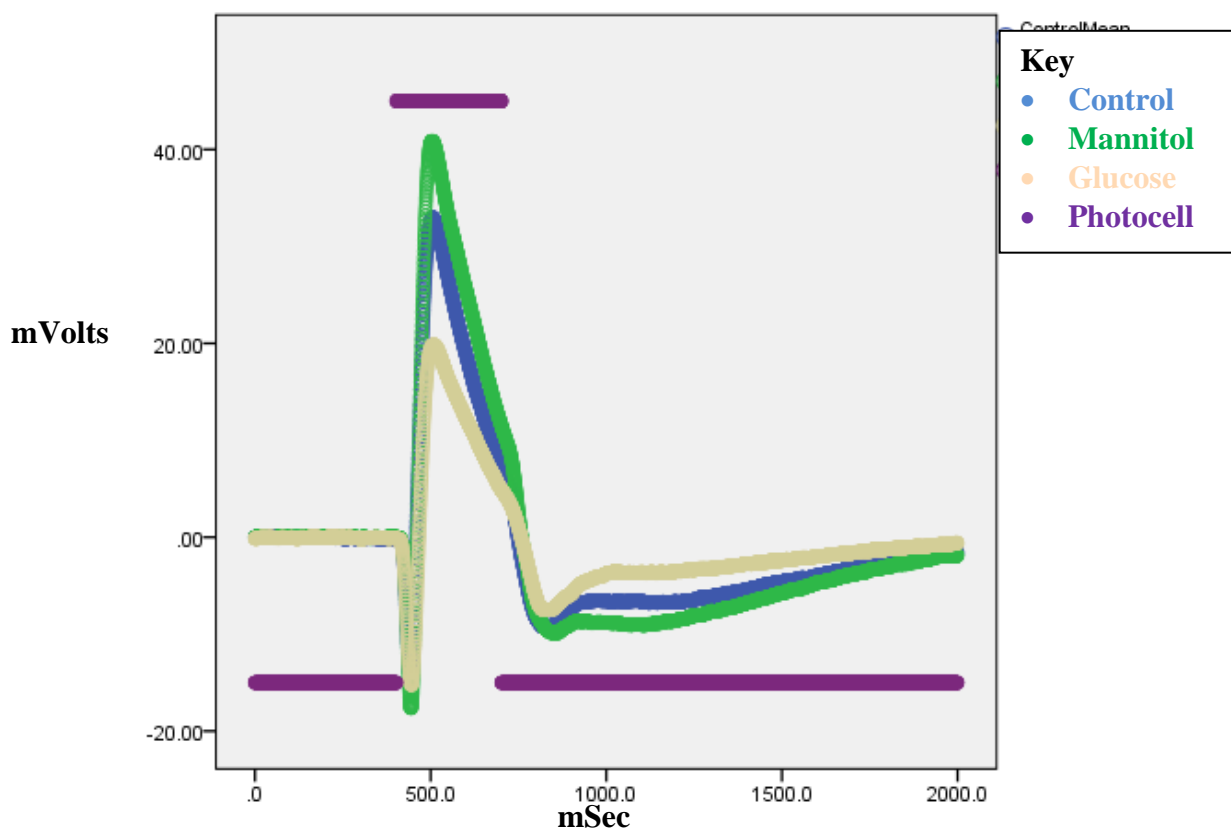


Figure 11. Mean ERG Responses to 570nm Stimulus for all Glucose, Mannitol, and Water Treated Retinas, ND 2.0, Blue Background. For each treatment group, the mean ERG response to a 570nm stimulus at 2.0 neutral density (ND) with a blue adapting (418nm) background were plotted together. Each treatment group contains 9 retinas from separate fish. The mean ERG response from glucose-treated, mannitol-treated, and water control are seen in grey, green, and blue, respectively. The figure shows a clear decrease in b-wave amplitude in glucose-treated retinal responses (43.5% reduction). Mean mannitol-treated retinal response seems to be almost exactly the same as mean water-control retinal response; however, the mannitol group peaks slightly higher (13.5% higher).

Table 1

*Mean a- and b-wave Amplitudes for a 570nm Stimulus and Percent Change from Water Control for Mannitol and Glucose Treatment Groups, Blue Background*

Treatment	a-wave Peak Amplitude $\pm$ SE (mV)	% change in a-wave amplitude	b-wave peak amplitude $\pm$ SE (mV)	% change in b-wave amplitude
Water Treated	$-18.6 \pm 2.4$	-	$35.9 \pm 7.5$	-
Manitol Treated	$-22.3 \pm 3.5$	20.0%	$40.7 \pm 5.9$	13.5%
Glucose Treated	$-19.0 \pm 2.3$	2.6%	$20.4 \pm 3.9$	43.3%

*Note.* a- and b-wave peak amplitudes on mean ERG plots for the three treatment groups (glucose-treated, manitol-treated, and water control) when exposed to a 570nm stimulus with a blue background. % changes in both a- and b-wave are displayed for the glucose and manitol treatment groups in comparison to the water control..

The mean ERG response to a 570nm stimulus on a red adapting background (Figure 12) is almost identical to the mean response recorded on a blue-adapting background. The three treatment groups had the same waveform, all with the same timing and latency; no responses were delayed. b-wave amplitude for the glucose treatment group was also reduced by 35.6% when compared the other two controls, which were almost identical (Table 2).



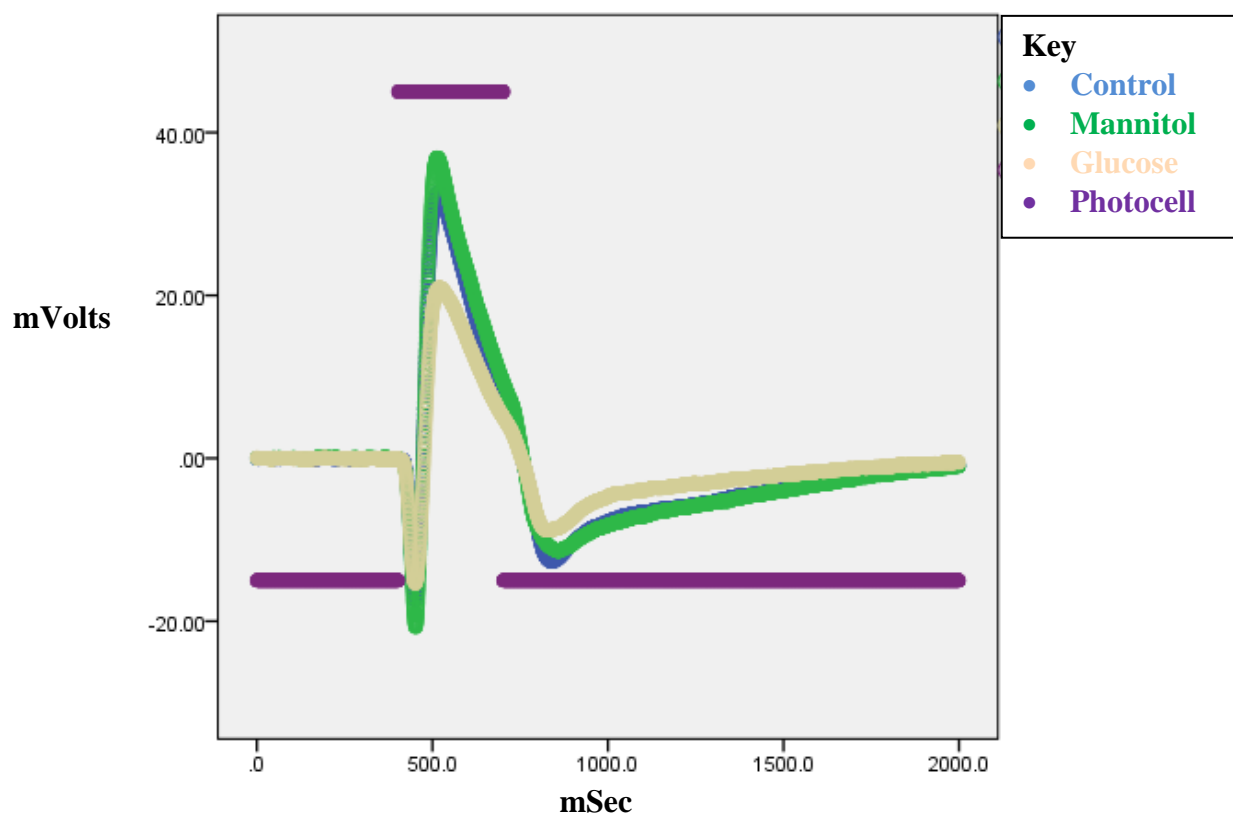


Figure 12. Mean ERG Responses to 570nm Stimulus for all Glucose, Mannitol, and Water Treated Retinas, ND 2.0, Red Background. For each treatment group, the mean ERG response to a 570nm stimulus at 2.0 neutral density (ND) with a red adapting (627nm) background were plotted. Each treatment group contains 9 retinas from separate fish. The mean ERG response from glucose-treated, manitol-treated, and water control are seen in grey, green, and blue, respectively. The figure shows a clear decrease in b-wave amplitude (-35.6% reduction) in the mean glucose-treated retinal response. Mean mannitol-treated retinal response seems to be almost exactly the same as mean water-control retinal response.

Table 2

*Mean a- and b-wave Amplitudes for a 570nm Stimulus and Percent Change from Water Control for Mannitol and Glucose Treatment Groups, Red Background*

Treatment	a-wave Peak Amplitude $\pm$ SE (mV)	% change in a-wave amplitude	b-wave peak amplitude $\pm$ SE (mV)	% change in b-wave amplitude
Water Treated	-20.6 $\pm$ 3.4	-	34.5 $\pm$ 6.9	-
Manitol Treated	-23.2 $\pm$ 3.3	12.8%	36.0 $\pm$ 5.5	4.4%
Glucose Treated	-18.9 $\pm$ 2.5	8.0%	22.2 $\pm$ 3.6	35.6%

*Note.* a- and b-wave peak amplitudes on mean ERG plots for the three treatment groups (glucose-treated, manitol-treated, and water control) when exposed to a 570nm stimulus with a red background. % changes in both a- and b-wave are displayed for the glucose and manitol treatment groups in comparison to the water control.

The mean ERG responses to the 490nm stimulus (close to the  $\lambda_{\text{max}}$  for the blue cone opsin) recorded with a blue adapting background (Figure 13) also showed the same overall waveform for all three treatment groups. a- and b-wave amplitudes were reduced in the glucose treated group compared to both control responses. The b-wave amplitude was reduced by 37.0% compared to the water control as noted in Table 3. None of the responses were delayed.

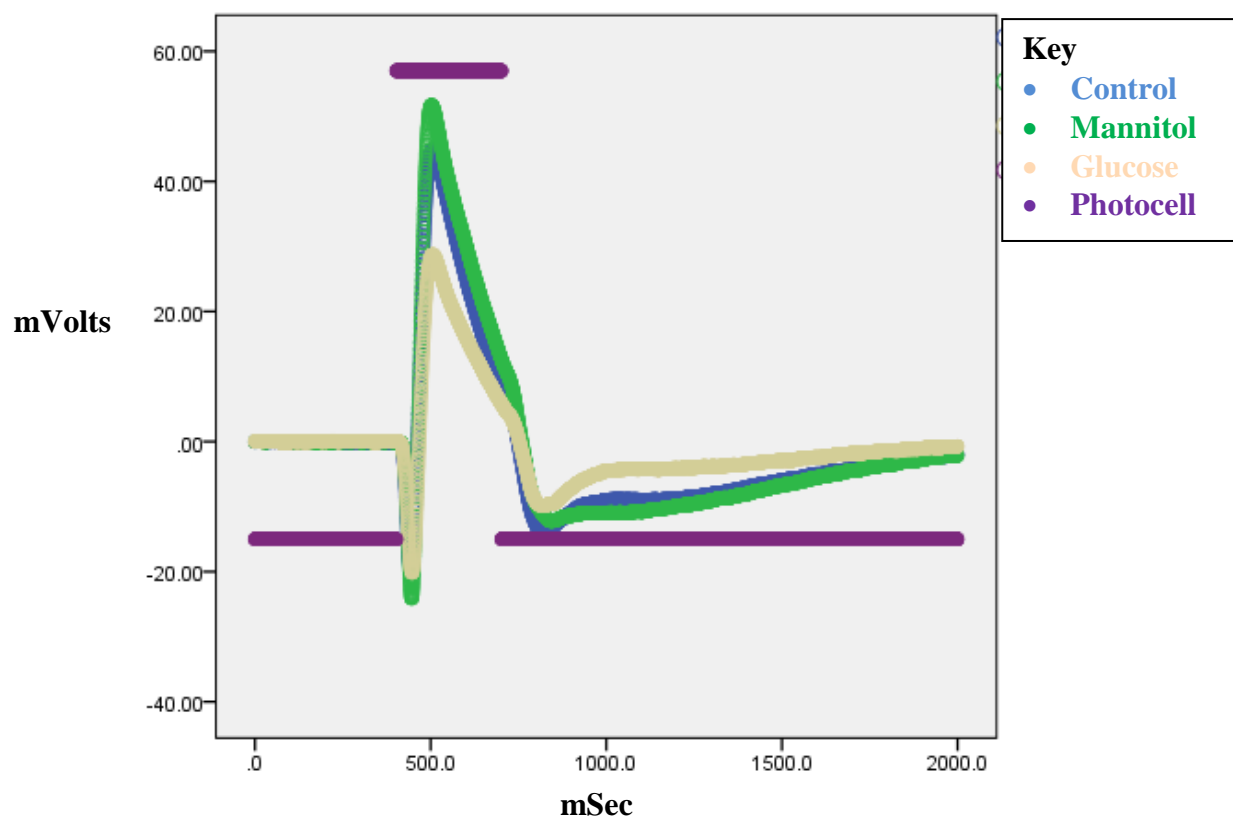


Figure 13. Mean ERG Responses to 490nm Stimulus for all Glucose, Mannitol, and Water Treated Retinas, ND 2.0, Blue Background. For each treatment group, the mean ERG response to a 490nm stimulus at 2.0 neutral density (ND) with a blue (418nm) adapting background were plotted. Each treatment group contains 9 retinas from separate fish. The mean ERG response from glucose-treated, mannitol-treated, and water control are seen in grey, green, and blue, respectively. The figure shows a clear decrease in b-wave amplitude (37.0% reduction) in the mean glucose-treated retinal responses. Mean mannitol-treated retinal response seems to be almost exactly the same as mean water-control retinal response; however, the mannitol group peaks slightly higher (8.6% increase).

Table 3

*Mean a- and b-wave Amplitudes for a 490nm Stimulus and Percent Change from Water Control for Mannitol and Glucose Treatment Groups, Blue Background*

Treatment	a-wave Peak Amplitude $\pm$ SE (mV)	% change in a-wave amplitude	b-wave peak amplitude $\pm$ SE (mV)	% change in b-wave amplitude
Water Treated	-25.5 $\pm$ 3.2	-	47.5 $\pm$ 9.3	-
Manitol Treated	-30.2 $\pm$ 4.5	18.5%	51.0 $\pm$ 7.1	8.6%
Glucose Treated	-24.5 $\pm$ 2.9	3.8%	29.9 $\pm$ 3.7	37.0%

*Note.* a- and b-wave peak amplitudes on mean ERG plots for the three treatment groups (glucose-treated, manitol-treated, and water control) when exposed to a 490nm stimulus with a blue background. % changes in both a- and b-wave are displayed for the glucose and manitol treatment groups in comparison to the water control.

Stimulating with 490nm of light on a red adapting background (Figure 14) gave similar results as seen with the blue adapting background: a similar overall waveform and reduced a- and b-wave amplitudes in glucose-treated retinas. b-wave amplitudes in glucose-treated retinas were reduced by 36.8% as seen in Table 4. No delay in onset of response was noted for any treatment groups.

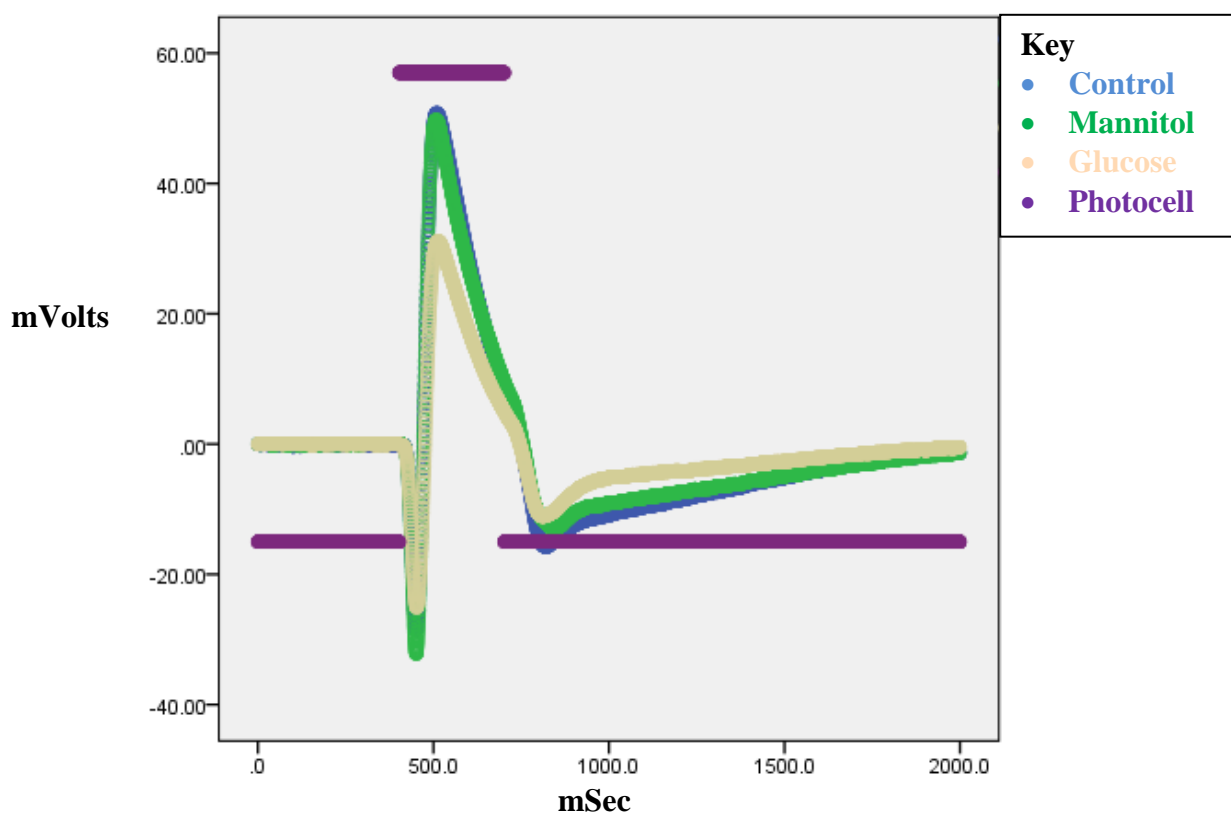


Figure 14. Mean ERG Responses to 490nm Stimulus for all Glucose, Mannitol, and Water Treated Retinas, ND 2.0, Red Background. For each treatment group, the mean ERG response to a 490nm stimulus at 2.0 neutral density (ND) with a red (627nm) adapting background stimulus were plotted. Each treatment group contains 9 retinas from separate fish. The mean ERG response from glucose-treated, mannitol-treated, and water control are seen in grey, green, and , respectively. The figure shows a decrease in b-wave amplitude (36.8% reduction) in mean glucose-treated retinal response. Mean mannitol-treated retinal response seems to be almost exactly the same as mean water-control retinal response.

Table 4

*Mean a- and b-wave Amplitudes for a 490nm Stimulus and Percent Change from Water Control for Mannitol and Glucose Treatment Groups, Red Background*

Treatment	a-wave Peak Amplitude $\pm$ SE (mV)	% change in a-wave amplitude	b-wave peak amplitude $\pm$ SE (mV)	% change in b-wave amplitude
Water Treated	-30.6 $\pm$ 4.2	-	52.3 $\pm$ 9.8	-
Manitol Treated	-35.6 $\pm$ 4.4	16.1%	49.4 $\pm$ 6.7	5.4%
Glucose Treated	-30.0 $\pm$ 3.8	2.1%	33.0 $\pm$ 5.0	36.8%

*Note.* a- and b-wave peak amplitudes on mean ERG plots for the three treatment groups (glucose-treated, manitol-treated, and water control) when exposed to a 490nm stimulus with a red background. % changes in both a- and b-wave are displayed for the glucose and manitol treatment groups in comparison to the water control.

The largest reduction in mean ERG response of b-wave amplitude was seen in response to the 410nm stimulus (near the  $\lambda_{\text{max}}$  for green cone opsin). Using a blue adapting background (Figure 15) there was a reduction in a- and b-wave amplitudes in glucose-treated retinas. b-wave amplitude is reduced by 42.8% in glucose-treated retinas (Table 5). Similar reductions in a- and b-wave amplitude were also seen in the mean ERG responses to the 410nm stimulus with a red adapting background (Figure 16). b-wave amplitudes for glucose-treated fish were reduced by 43.1% (Table 6). No delay in response onset was observed.

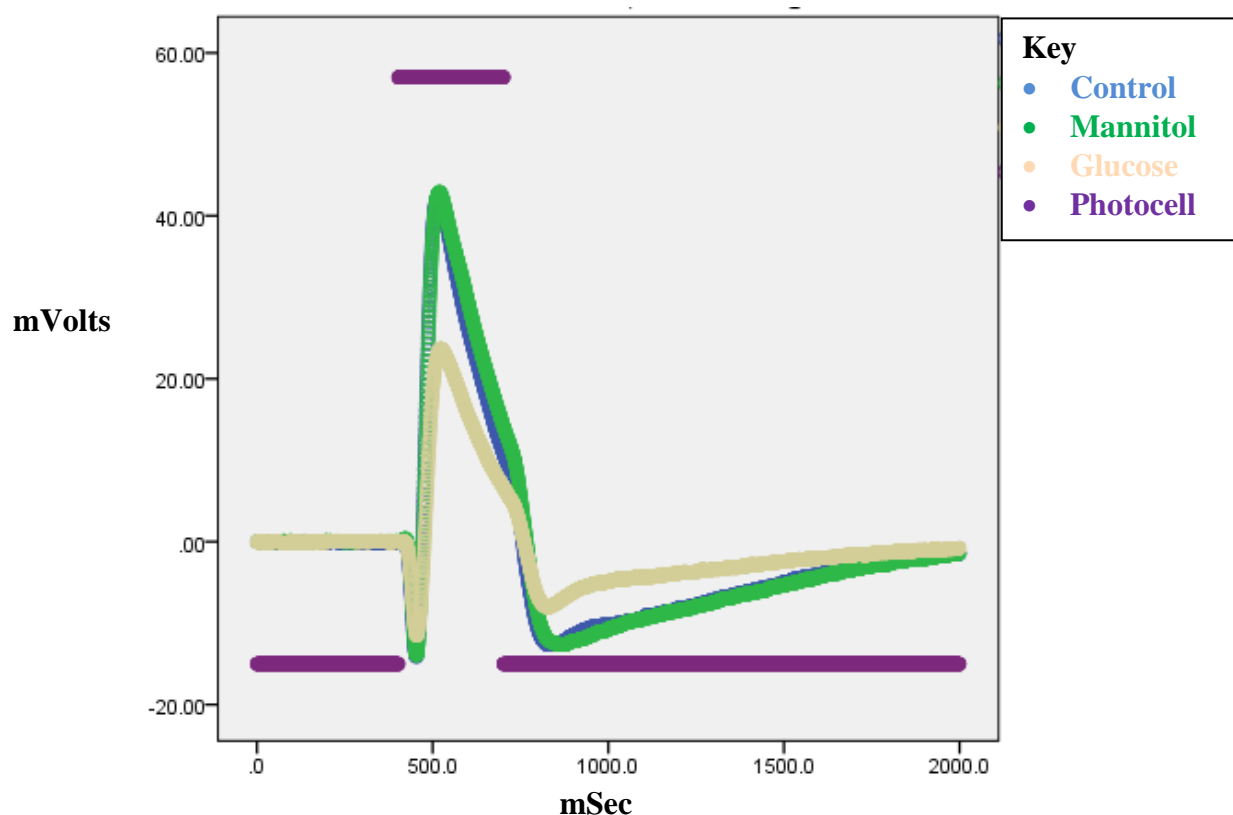


Figure 15. Mean ERG Responses to 410nm Stimulus for all Glucose, Mannitol, and Water Treated Retinas, ND 2.0, Blue Background. For each treatment group, the mean ERG response to a 410nm stimulus at 2.0 neutral density (ND) with a blue (418nm) adapting background stimulus were plotted. Each treatment group contains 9 retinas from separate fish. The mean ERG response from glucose-treated, mannitol-treated, and water control are seen in grey, green, and blue, respectively. The figure shows a decrease in b-wave amplitude (42.8% reduction) in the mean glucose-treated retinal response. Mean mannitol-treated retinal response seems to be almost exactly the same as mean water-control retinal response.

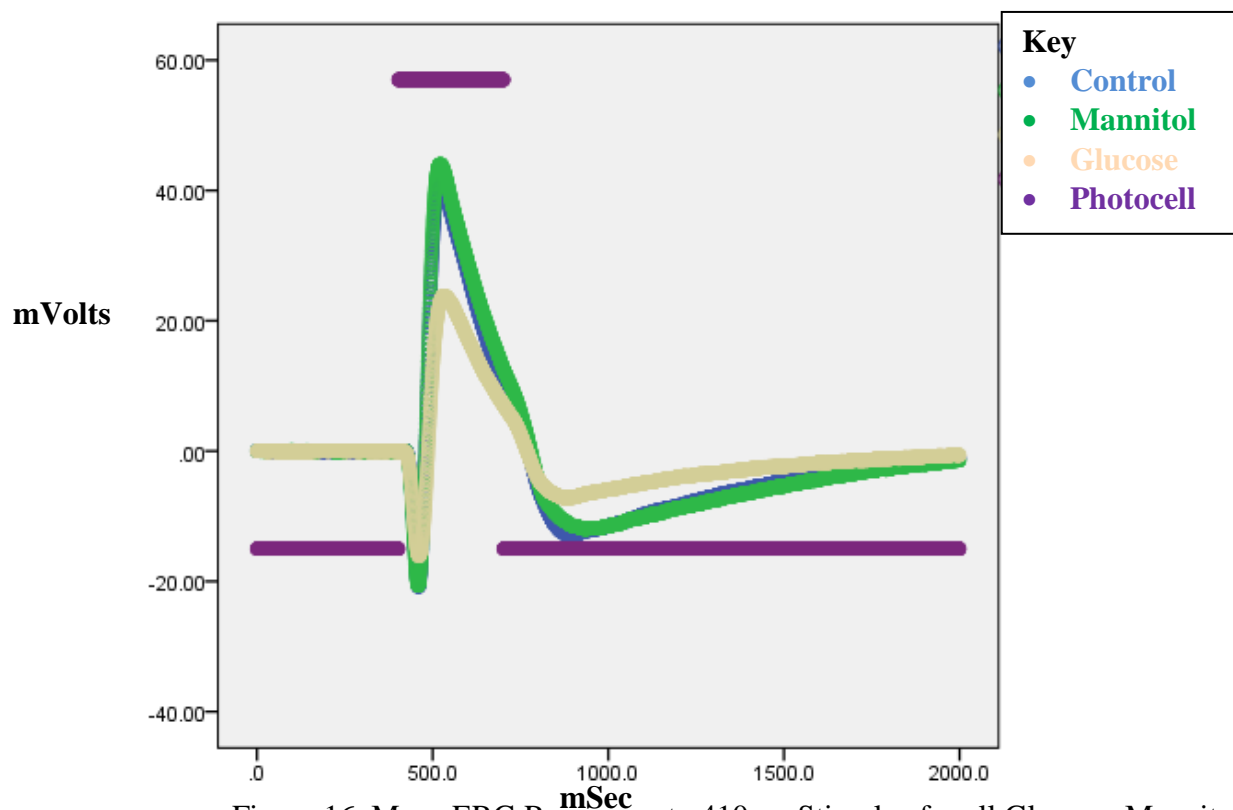


Figure 16. Mean ERG Responses to 410nm Stimulus for all Glucose, Mannitol, and Water Treated Retinas, ND 2.0, Red Background. For each treatment group, the mean ERG response to a 410nm stimulus at 2.0 neutral density (ND) with a red (627nm) adapting background stimulus were plotted. Each treatment group contains 9 retinas from separate fish. The mean ERG response from glucose-treated, mannitol-treated, and water control are seen in grey, green, and blue, respectively. The figure shows a decrease in b-wave amplitude (43.1% reduction) in the mean glucose-treated retinal response. Mean mannitol-treated retinal response seems to be almost exactly the same as mean water-control retinal response.



Table 5

*Mean a- and b-wave Amplitudes for a 410nm Stimulus and Percent Change from Water Control for Mannitol and Glucose Treatment Groups, Blue Background*

Treatment	a-wave Peak Amplitude $\pm$ SE (mV)	% change in a-wave amplitude	b-wave peak amplitude $\pm$ SE (mV)	% change in b-wave amplitude
Water Treated	-18.5 $\pm$ 3.1	-	41.8 $\pm$ 9.2	-
Manitol Treated	-21.3 $\pm$ 3.4	14.9%	42.9 $\pm$ 7.2	2.0%
Glucose Treated	-15.0 $\pm$ 2.2	19.2%	23.8 $\pm$ 3.5	42.8%

*Note.* a- and b-wave peak amplitudes on mean ERG plots for the three treatment groups (glucose-treated, manitol-treated, and water control) when exposed to a 410nm stimulus with a blue background. % changes in both a- and b-wave are displayed for the glucose and manitol treatment groups in comparison to the water control.

Table 6

*Mean a- and b-wave Amplitudes for a 410nm Stimulus and Percent Change from Water Control for Mannitol and Glucose Treatment Groups, Red Background*

Treatment	a-wave Peak Amplitude $\pm$ SE (mV)	% change in a-wave amplitude	b-wave peak amplitude $\pm$ SE (mV)	% change in b-wave amplitude
Water Treated	-22.2 $\pm$ 3.9	-	42.9 $\pm$ 8.4	-
Manitol Treated	-24.6 $\pm$ 3.6	10.9%	43.6 $\pm$ 6.9	1.7%
Glucose Treated	-19.3 $\pm$ 2.9	12.5%	24.4 $\pm$ 4.0	43.1%

*Note.* a- and b-wave peak amplitudes on mean ERG plots for the three treatment groups (glucose-treated, manitol-treated, and water control) when exposed to a 410nm stimulus with a red background. % changes in both a- and b-wave are displayed for the glucose and manitol treatment groups in comparison to the water control.

The mean ERG responses to the 370nm stimulus (near the  $\lambda_{\text{max}}$  for the UV cone opsin) with a blue adapting background (Figure 17) shows there is no discrepancy in onset of the wave. However, a-wave and b-wave amplitudes are reduced in the glucose treatment group compared to the mannitol and water control groups. The mean b-wave amplitude was reduced by 32.7% in glucose treated retinas (Table 7). This is mirrored in the mean ERG responses to the 370nm stimulus with a red adapting background (Figure 18). The reduction in b-wave amplitude of the mean glucose-treated retinas is 42.5% when compared to water control (Table 8).

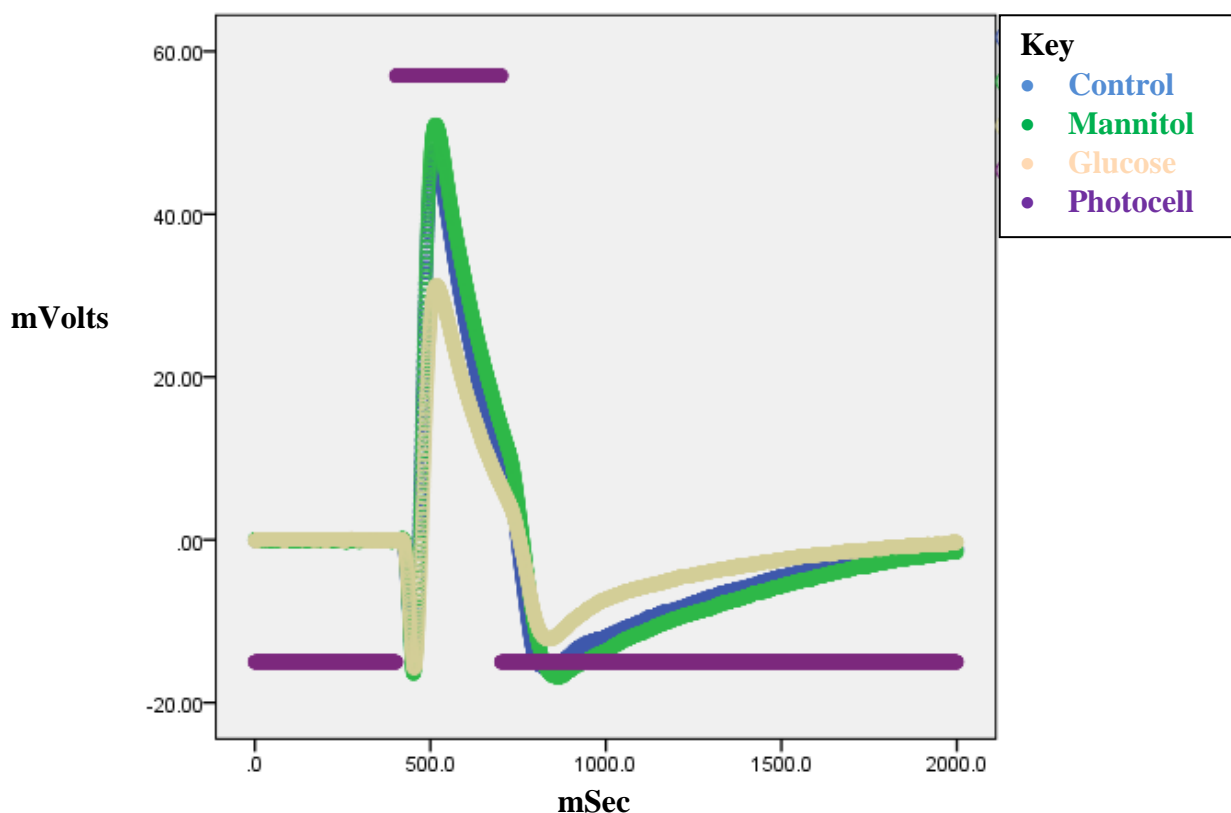


Figure 17. Mean ERG Responses to 370nm Stimulus for all Glucose, Mannitol, and Water Treated Retinas, ND 2.0, Blue Background. Each treatment group contains 9 retinas from separate fish. The mean ERG response from glucose-treated, mannitol-treated, and water control are seen in grey, green, and blue, respectively. The figure shows a decrease in b-wave amplitude (32.7% reduction) in the mean glucose-treated retinal response. Mean mannitol-treated retinal response seems to be almost exactly the

same as mean water-control retinal response; however, the mean mannitol-treated response seems to peak higher than that of the water controls (10.0%).

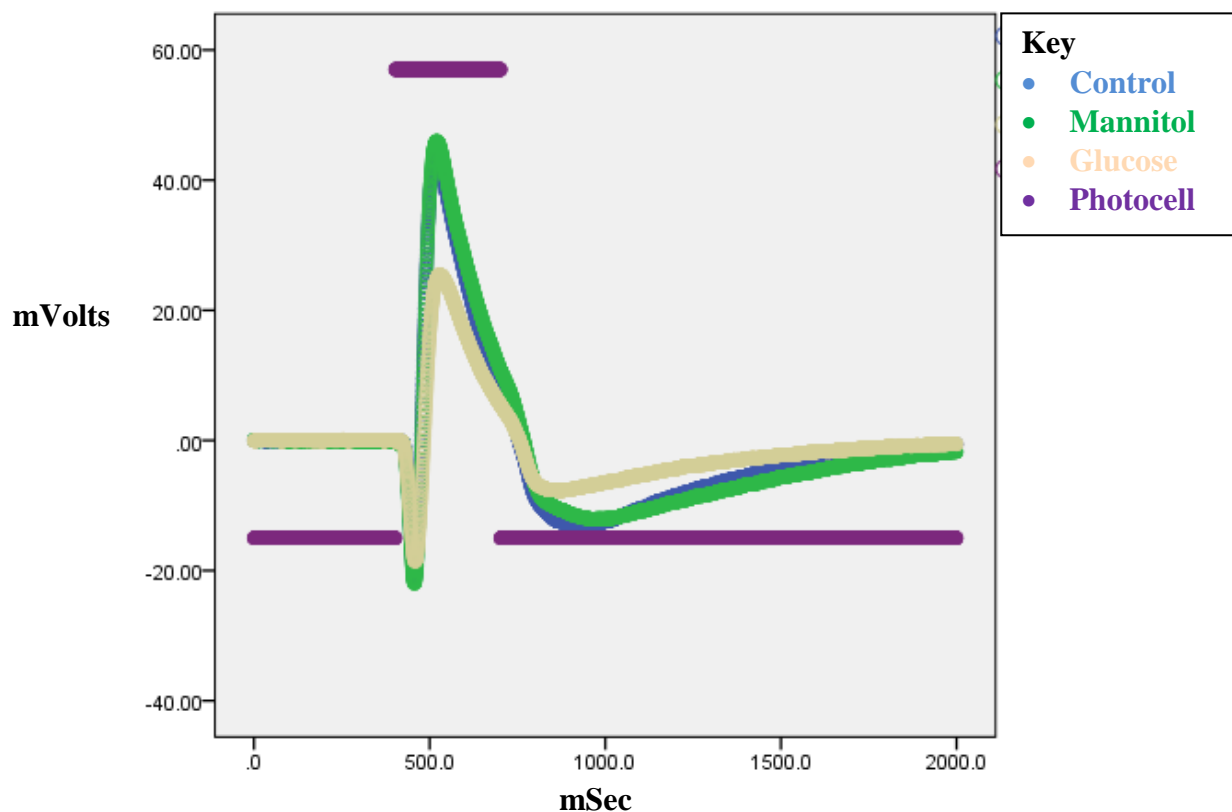


Figure 18. Mean ERG Responses to 370nm Stimulus for all Glucose, Mannitol, and Water Treated Retinas, ND 2.0, Red Background. For each treatment group, the mean ERG response to a 370nm stimulus at 2.0 neutral density (ND) with a red (627nm) adapting background stimulus were plotted. Each treatment group contains 9 retinas from separate fish. The mean ERG response from glucose-treated, mannitol-treated, and water control are seen in grey, green, and blue, respectively. The figure shows a decrease in b-wave amplitude in the mean glucose-treated retinal response (42.5% reduction). Mean mannitol-treated retinal response seems to be almost exactly the same as mean water-control retinal response.

Table 7

*Mean a- and b-wave Amplitudes for a 370nm Stimulus and Percent Change from Water Control for Mannitol and Glucose Treatment Groups, Blue Background*

Treatment	a-wave Peak Amplitude $\pm$ SE (mV)	% change in a-wave amplitude	b-wave peak amplitude $\pm$ SE (mV)	% change in b-wave amplitude
Water Treated	-19.4 $\pm$ 3.3	-	46.3 $\pm$ 10.4	-
Manitol Treated	-23.3 $\pm$ 3.6	20.3%	50.9 $\pm$ 8.3	10.0%
Glucose Treated	-19.3 $\pm$ 2.9	3.5%	31.1 $\pm$ 5.0	32.7%

*Note.* a- and b-wave peak amplitudes on mean ERG plots for the three treatment groups (glucose-treated, manitol-treated, and water control) when exposed to a 370nm stimulus with a blue background. % changes in both a- and b-wave are displayed for the glucose and manitol treatment groups in comparison to the water control.

Table 8

*Mean a- and b-wave Amplitudes for a 370nm Stimulus and Percent Change from Water Control for Mannitol and Glucose Treatment Groups, Red Background*

Treatment	a-wave Peak Amplitude $\pm$ SE (mV)	% change in a-wave amplitude	b-wave peak amplitude $\pm$ SE (mV)	% change in b-wave amplitude
Water Treated	-22.4 $\pm$ 4.0	-	45.2 $\pm$ 9.9	-
Manitol Treated	-25.1 $\pm$ 3.4	11.9%	45.6 $\pm$ 7.3	0.9%
Glucose Treated	-20.8 $\pm$ 3.3	6.7%	25.6 $\pm$ 4.6	42.5%

*Note.* a- and b-wave peak amplitudes on mean ERG plots for the three treatment groups (glucose-treated, manitol-treated, and water control) when exposed to a 370nm stimulus with a red background. % changes in both a- and b-wave are displayed for the glucose and manitol treatment groups in comparison to the water control.

The last individual wavelength examined was the 650nm (far-red) stimulus with a neutral density of 1.5. The neutral density of 1.5 was used because the photoreceptors are less sensitive to this wavelength and, consequently, a slightly brighter stimulus needs to be used to elicit a response. This is the brightest intensity at this wavelength that elicited a consistent response. Using the blue adapting background, the mean ERG responses to the 650nm stimulus (Figure 19) shows a response that was unique from the responses elicited by the other stimulating wavelengths. The overall waveform and onset of response between groups is the same; however, the mannitol treatment group has the largest a- and b-wave response amplitudes (40.0% and 62.1% increase when compared to water control (Table 9)). While the water control and glucose treatment groups seemed to have similar (and smaller) a- and b-wave amplitudes. Mean b-wave amplitude for the glucose treatment group was 10.4% reduced when compared to water control (Table 10).

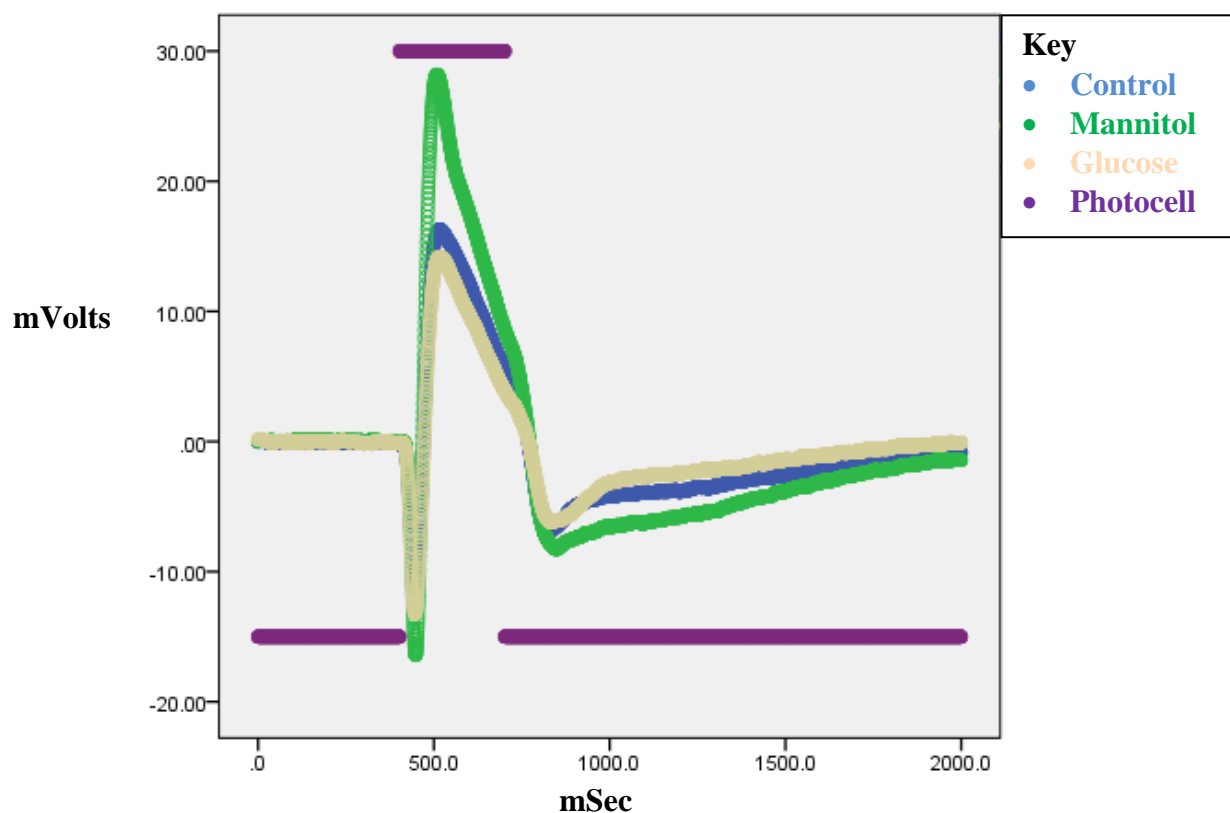


Figure 19. Mean ERG Responses to 650nm Stimulus for all Glucose, Mannitol, and Water Treated Retinas, ND 1.5, Blue Background. For each treatment group, the mean ERG response to a 650nm stimulus at 1.5 neutral density (ND) with a blue (418) adapting background stimulus were plotted. Each treatment group contains 9 retinas from separate fish. The mean ERG response from glucose-treated, mannitol-treated, and water control are seen in grey, green, and blue, respectively. The figure shows a decrease in b-wave amplitude in the mean glucose-treated retinal response compared to the water control response (10.4% reduction). The mean mannitol-treated retinal response seems to be larger than both other treatment groups (62.1% larger than the water control).

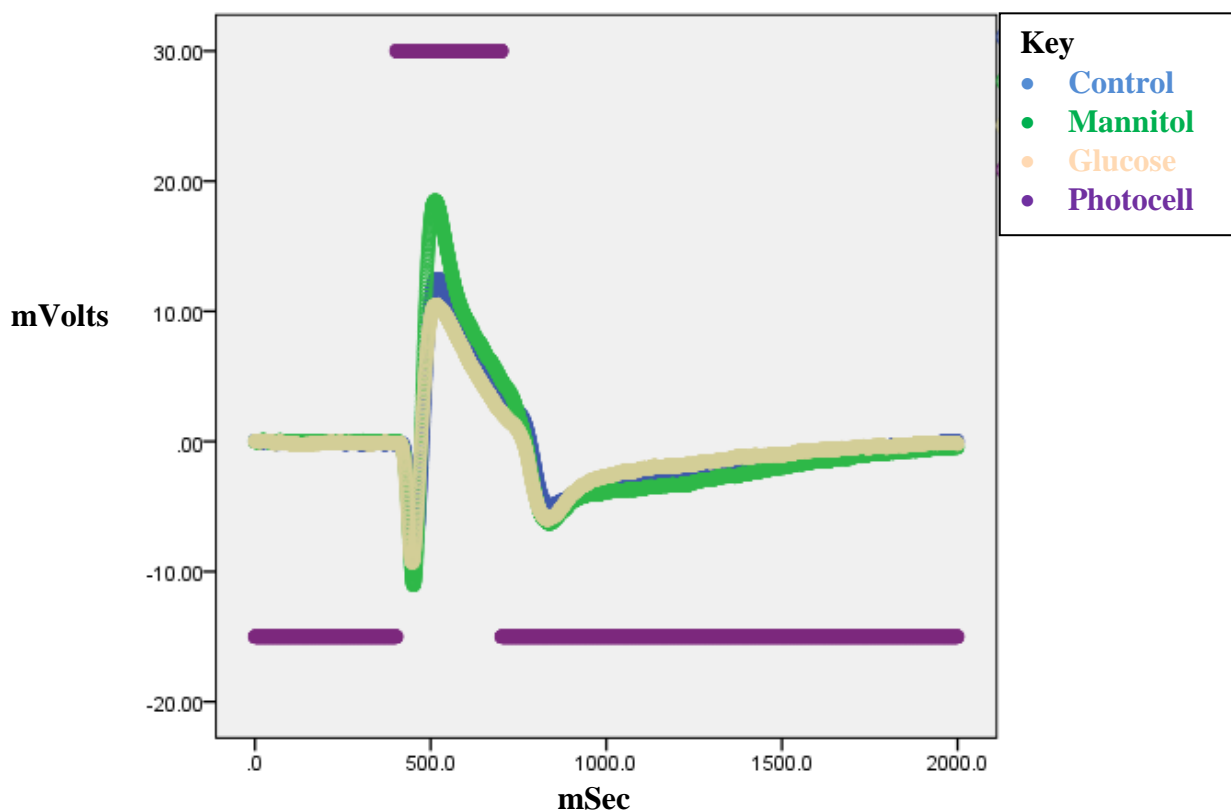


Figure 20. Mean ERG Responses to 650nm Stimulus for all Glucose, Mannitol, and Water Treated Retinas, ND 1.5, Red Background. For each treatment group, the mean ERG response to a 650nm stimulus at 1.5 neutral density (ND) with a red (627) adapting background stimulus were plotted. Each treatment group contains 9 retinas from separate fish. The mean ERG response from glucose-treated, mannitol-treated, and water control are seen in grey, green, and blue, respectively. The figure shows a decrease in b-wave amplitude in the mean glucose-treated retinal response compared to the water control response (17.7%). The mean mannitol-treated retinal response seems to be larger than both other treatment groups (27.5% larger than the water control).

Table 9

*Mean a- and b-wave Amplitudes for a 650nm Stimulus and Percent Change from Water Control for Mannitol and Glucose Treatment Groups, Blue Background*

Treatment	a-wave Peak Amplitude $\pm$ SE (mV)	% change in a-wave amplitude	b-wave peak amplitude $\pm$ SE (mV)	% change in b-wave amplitude
Water Treated	-13.8 $\pm$ 2.3	-	16.7 $\pm$ 2.3	-
Manitol Treated	-19.4 $\pm$ 2.7	40.0%	27.1 $\pm$ 4.0	62.1%
Glucose Treated	-16.6 $\pm$ 2.2	20.2%	14.9 $\pm$ 2.5	10.4%

*Note.* a- and b-wave peak amplitudes on mean ERG plots for the three treatment groups (glucose-treated, manitol-treated, and water control) when exposed to a 650nm stimulus with a blue background. % changes in both a- and b-wave are displayed for the glucose and manitol treatment groups in comparison to the water control.

Table 10

*Mean a- and b-wave Amplitudes for a 650nm Stimulus and Percent Change from Water Control for Mannitol and Glucose Treatment Groups, Red Background*

Treatment	a-wave Peak Amplitude $\pm$ SE (mV)	% change in a-wave amplitude	b-wave peak amplitude $\pm$ SE (mV)	% change in b-wave amplitude
Water Treated	-9.5 $\pm$ 1.9	-	13.6 $\pm$ 2.4	-
Manitol Treated	-13.3 $\pm$ 1.9	39.1%	17.4 $\pm$ 2.7	27.5%
Glucose Treated	-11.7 $\pm$ 1.9	22.7%	11.2 $\pm$ 2.4	17.7%

*Note.* a- and b-wave peak amplitudes on mean ERG plots for the three treatment groups (glucose-treated, manitol-treated, and water control) when exposed to a 650nm stimulus with a red background. % changes in both a- and b-wave are displayed for the glucose and manitol treatment groups in comparison to the water control.



For the red adapting background, the mean ERG responses to the 650nm stimulus again showed the response of mannitol treated retinas to have a higher overall a- and b-wave amplitude when compared to either water control or glucose treated groups. Further, the glucose-treated group had smaller a- and b-wave amplitudes when compared to the water control groups. b-wave mean amplitude for the glucose-treated group was reduced by 17.7% when compared to water control. When comparing the mean responses to a 650nm stimulus with the different adapting backgrounds, the higher mannitol-group response amplitude was reduced when exposed to the red adapting background.

Figures 21 and 22 show the mean ( $\pm$  SE) maximum b-wave amplitude for each treatment group when stimulated with various wavelengths (570nm, 490nm, 410nm, and 370nm) at 2.0 ND with a blue and red background, respectively. The glucose treatment group clearly shows a reduced amplitude at each of the four wavelengths when exposed to both a red and background stimulus.

Statistical analysis shows a significant difference in the b-wave maximum amplitude recorded in the glucose treatment group compared to the control group at three of the stimulating wavelengths: 570nm ( $p = 0.031, 0.049$ ), 490nm ( $p = 0.041, 0.045$ ), and 410nm ( $p = 0.039, 0.028$ ) for both a red and blue background, respectively. The comparison of means conducted between the two groups at the 370nm wavelength stimulus with a red background was also significant, with a p-value of 0.04; however, the comparison of means for the maximum b-wave amplitude at 370nm wavelength stimulus with a blue background was not significantly different ( $p = 0.09$ ). No significant

differences in mean b-wave current amplitude in response to a 650nm stimulus were observed using either background color ( $p = 0.31$  for red background;  $p = 0.24$  for blue background).

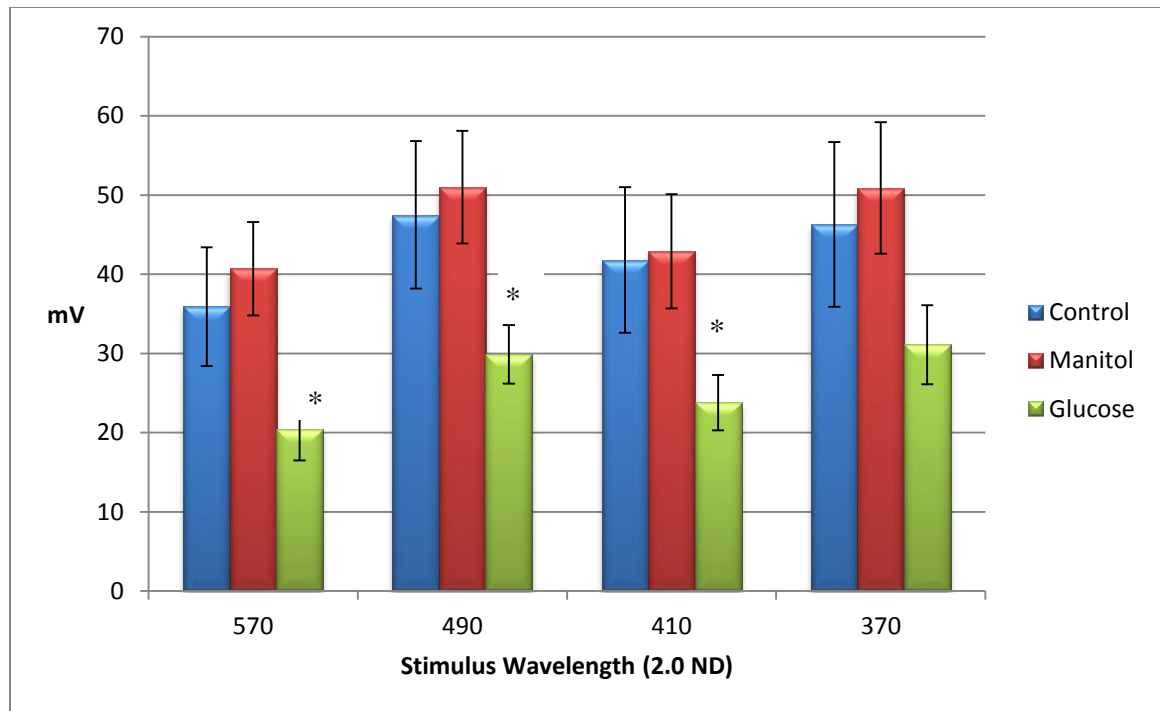


Figure 21. Mean B-Wave Amplitude Comparison at Individual Wavelengths for All Treatment Groups, Blue Background. Histogram showing the mean maximum amplitude of the b-wave for each treatment group at light stimuli with following wavelengths: 570nm, 490nm, 410nm, and 370nm. A total of nine retinas were used for each treatment group. A red (627nm) background stimulus was used. Glucose-treated retinas seemed to have a smaller mean b-wave amplitude when compared to controls. \* indicates that the mean b-wave amplitude for the glucose treated group was statistically significantly lower than the mean b-wave amplitude for the water control.

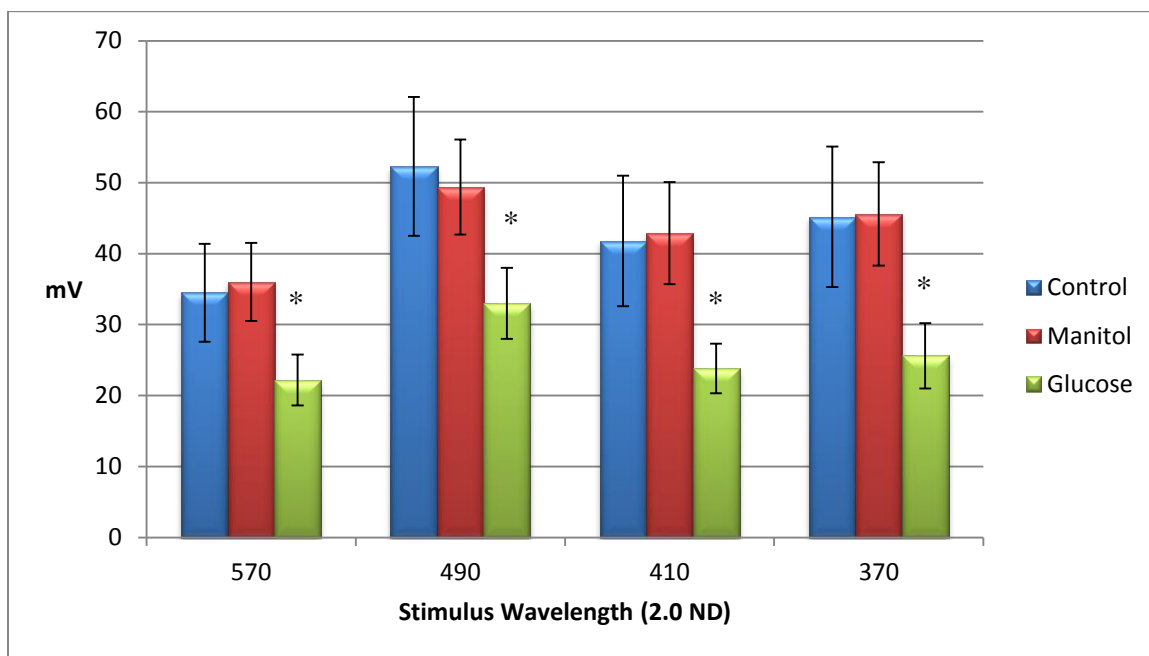


Figure 22. Mean B-Wave Amplitude Comparison at Individual Wavelengths for all Treatment Groups, Red Background. Histogram showing the mean maximum amplitude of the b-wave for each treatment group at light stimuli with following wavelengths: 570nm, 490nm, 410nm, and 370nm. A total of nine retinas were used for each treatment group. A red (627nm) background stimulus was used. Glucose-treated retinas seemed to have a smaller mean b-wave amplitude when compared to controls. \* indicates that the mean b-wave amplitude for the glucose treated group was statistically significantly lower than the mean b-wave amplitude for the water control.

### Software-Generated Spectral Analysis

Using a spectral model (Connaughton and Nelson, 2010; Nelson and Singla, 2009), contributions of the different cone photoreceptor types to the ERG responses were determined. To do this, a spectral analysis for each set of ERG recordings created a variable for each cone type representing the highest sensitivity of that cone type. Sensitivity was determined by calculating trough to peak response amplitudes for each wavelength and then comparing the observed response with a software-generated expected response for each wavelength. The resulting four response variables,  $V_r$ ,  $V_g$ ,  $V_b$ , and  $V_u$  represent the peak sensitivity of each respective cone type (red, green, blue, and

UV) observed for each ERG recording.  $R^2$  values indicate the individual fit of the recorded ERG with the expected waveform.

Response variables were calculated for the mean ERG responses to each stimulating wavelength elicited using both with the blue adapting background (Table 11) and the red adapting background (Table 12). There was no discernible pattern in the mean response variables between the three treatment groups either adapting background.

Table 11

*Mean Spectral Response Variable Comparison for all Three Treatment Groups, Blue Background*

Variable	Control Mean	Mannitol Mean	Glucose Mean
Vr	41.6	49.9	35.8
Vg	20.1	36.7	31.5
Vb	32.5	26.8	16.7
Vu	32.3	42.7	53.7
R2	0.924	0.967	0.952

*Note.* Averaged spectral response variables calculated from each treatment group's ERGs taken using a blue adapting background. Each treatment group contains 9 retinas from separate fish. Software-computed trough-peak sensitivity was analyzed and resulting variables indicate peak sensitivity for red cones (Vr), green cones (Vg), blue cones (Vb), and UV cones (Vu). R2 values represent waveform fit to the expected model. As can be seen in the table, no resulting pattern is discernable between treatment groups. For water controls: red cone inputs were 2x green cone inputs, while blue and UV cone inputs were similar. In mannitol treated retinas, red and UV cone contributions were the largest, while blue cone inputs were the smallest. In glucose treated retinas, UV cone contributions are largest, red and green cone inputs are similar and blue cone inputs are the least.

Table 12

*Mean Spectral Response Variable Comparison for all Three Treatment Groups, Red Background*

Variable	Control Mean	Mannitol Mean	Glucose Mean
Vr	41.1	36.6	36.0
Vg	38.1	44.3	40.4
Vb	22.7	13.2	12.0
Vu	32.0	13.1	33.2
R2	0.964	0.976	0.977

*Note.* Averaged spectral response variables calculated from each treatment group's ERGs taken with a red adapting background. Each treatment group contains 9 retinas from separate fish. Software-computed trough-peak sensitivity was analyzed and resulting variables indicate peak sensitivity for red cones (Vr), green cones (Vg), blue cones (Vb), and UV cones (Vu).  $R^2$  values represent waveform fit to the expected model. As can be seen in the table, no resulting pattern is discernable between treatment groups

## CHAPTER 4

### DISCUSSION

Glucose-treated zebrafish retinas showed a marked reduction in photoreceptor and on-center bipolar cell functional responses as indicated by reduced a- and b-wave amplitudes. Amplitude reductions were observed in response to all stimulating wavelengths used (570nm, 490nm, 410nm, and 370nm) regardless of background stimulus color. A similar reduction in b-wave response was noted in the mean overall glucose-treated retinal ERG response (Figures 9 and 10).

As stated previously, the a-wave portion of the ERG response is known to correlate to photoreceptor activation. The b-wave portion of the ERG correlates to on-center bipolar cell activity and Muller cell responses. We were able to isolate these waveforms by using the glutamate receptor antagonist CNQX in the bath solution. CNQX blocks AMPA/kainate-type glutamate receptors as evidenced by the successful elimination of oscillatory potentials (OP) and d-waves in all recorded ERGs. In previous literature (Gleeson et al, 2006), it was established that a thinning of the inner retina, particularly the INL and IPL, occurs following one month of hyperglycemic conditions in zebrafish. Bipolar cell bodies are located in the INL and their axon terminals are located in the IPL. This suggested that changes in these two retinal layers may be due to a loss of bipolar cells, leading us to hypothesize that bipolar cell function, specifically ON-bipolar

cell function, may be altered in glucose-treated zebrafish retinas. The ERG results of this experiment fully support that hypothesis. The mean b-wave responses of the 9 glucose-treated retinas were consistently reduced when compared to those of both mannitol and water controls at all stimulating wavelengths of light used.

Previous studies report red cone loss after one month of hyperglycemic conditions in zebrafish (Alvarez, et al., 2010). To determine if other cone types are compromised in glucose-treated retinas, we stimulated the eyecups with varying wavelengths of light. The wavelengths chosen correspond to the peak-absorption wavelengths for each cone type: 570nm is the red cone peak, 480nm is the green cone peak, 415nm is the blue cone peak, and 360nm is the UV cone peak (Hughes, 1998). Previous data (Alvarez et al., 2010) has suggested that weakened ERG responses result from alterations in retinal cell morphology, often followed by degradation similar to what is seen in diabetic retinopathy patients.

Our findings support previous data (Alvarez et al., 2010), as we identified a reduction in b-wave amplitude when red cones were selectively stimulated. In addition, reductions in b-wave amplitude were also observed in glucose-treated retinas at the other stimulating wavelengths, suggesting some reduced functionality in green, blue, and UV cones (in addition to red cones) in treated animals (summarized in Figures 21 and 22). Wavelength-specific reductions in b-wave amplitude suggest that the decrease in ON-bipolar cell light responses may be due to a decreased functionality of ON-bipolar cells. It is important to note that mean a-wave responses were reduced in glucose treated retinas when compared to water control retinas. The reductions in a-wave amplitude were not as large as those seen in b-wave amplitude. Since the a-wave is correlated to photoreceptor

activity, it is also possible that reductions in b-wave are due to glucose-induced changes in photoreceptor cell activity. This finding is consistent with studies (Gleeson et al., 2006) showing thinning of the INL and IPL where ON-bipolar cells are located.

As an osmotic control, zebrafish were exposed to alternating 2% mannitol solutions. We do not believe our results are due to changes in osmotic conditions, because a- and b-wave amplitudes of mannitol-treated retinas are similar to amplitudes observed in water-treated retinas (see Figure 11 and 12). This was true for 570, 490, 410, and 370nm stimulating wavelengths, regardless of background stimulus color (Figures 13-20). Thus, the b-wave amplitude in glucose-treated animals is due to prolonged hyperglycemia and not osmotic stress.

The b-wave reductions in the glucose treatment group were larger by three or four times the a-wave reduction. This difference in a-wave and b-wave reductions could indicate photoreceptors are less sensitive to hyperglycemia than bipolar cells. This would indicate that bipolar cells are more severely affected by chronic high glucose levels than photoreceptors.

The only discrepancy observed in ERG responses across the individual stimulating wavelengths was observed in response to a 650nm stimulus (Figures 19, 20). In response to this stimulus, b-wave amplitudes in glucose-treated retinas were similar (but still reduced) to water-treated controls. Both of these responses were lower than b-wave amplitude recorded in mannitol-treated retinas. This suggests a strong effect of osmotic differences in this response. Based on the literature (Hughes, 1998), it seems that 650nm is on the border of the absorption spectrum for zebrafish cones. This wavelength is far-red light and would be located in the tail of the red cone response, stimulating few,



if any, red cones. Though the relationship between the treatment groups exposed to a 650nm stimulus is difficult to define, it may be a result that is specific to the effect of changes in osmotic pressure on red cones. Further investigation on zebrafish at this wavelength would need to occur before any conclusions could be drawn.

A total mean ERG response was plotted for each of the three treatment groups to look at any obvious trends. The overall waveform and specific a- and b-wave components observed at each stimulating wavelength were also apparent in the mean ERG response plot with both a blue background (Figure 9) and a red background (Figure 10); indicate the same relationship between the three treatment groups. The background stimuli were used in order to prevent the retina from dark adapting. Since using only one color for the background stimulus could skew the results, two separate wavelengths were used. The red background stimulus was thought to saturate red cone responses and the blue background stimulus was thought to saturate blue cone responses. Comparison of the two background wavelengths was hoped to provide additional information on reduced amplitudes, when specific cones had saturated responses. No patterned difference between the red and blue background stimuli was noted among the various wavelengths.

Last, the software-computed spectral response variables seen in Table 11 and Table 12 indicate no response pattern between the three groups. As can be seen in the tables, no resulting pattern is discernable between treatment groups. For water controls: red cone inputs were 2x green cone inputs, while blue and UV cone inputs were similar. In mannitol treated retinas, red and UV cone contributions were the largest, while blue cone inputs were the smallest. In glucose treated retinas, UV cone contributions are largest, red and green cone inputs are similar and blue cone inputs are the least. The lack

of pattern may be because the four variables computed by the software's spectral equation are creating values that are relative to one another. This is a problem because it suggests that parameter values may be unique to each ERG. Additionally, some data would have to be thrown out if the ERG response was too "noisy" to fit. However, with such a small n value (9 retinas per treatment group), throwing out data could reduce the statistical significance of the comparison between treatment groups if one was performed.

Clinically, individuals with diabetes, but no signs of diabetic retinopathy (i.e., no changes in retinal vasculature are noted), have shown changes in ERG responses. Consequently, irregular ERG recordings can function as an early sign of the progression of diabetic retinopathy. As stated previously, changes in OP amplitude are reported in diabetic patients with no other evidence of retinopathy (Ewing et al., 2009). Other irregular recordings indicate changes in the morphology of the retinal and eventual degradation of the retina (Alvarez et al., 2010). This experiment looked specifically at the b-wave and thus OP amplitudes were silenced by the presence of CNQX. Some studies (Papakostopoulos, 1996) have noted irregular ERG recordings such as reduced b-wave amplitudes in individuals who had developed diabetic retinopathy.

### **Conclusion**

Our data suggest that the reduced b-wave amplitudes of the glucose treatment group seen at various individual stimulating wavelengths as well as in an overall mean comparison indicate reduced functionality in on-center bipolar cells. This is consistent with previous finds (Alvarez et al., 2010) reporting reduced b- and d-wave amplitudes in hyperglycemic zebrafish and with anatomical studies showing a thinning of the inner

retina (Gleeson et al., 2007). Presumably, reduced retinal function occurs due to prolonged high glucose levels and not osmotic changes. Osmotic control and water control groups show no significant difference in a- or b-wave amplitude when compared to each other.

### **Future Research**

Physiological data characterized by ERG analysis, recorded from zebrafish retinas chronically exposed to chronic glucose treatment, show findings similar to those recorded from individuals with DR. The similarities in response support the use of zebrafish for future studies on diabetic retinopathy.

Future studies should focus on longer hyperglycemia treatment periods in order to create an even larger discrepancy between glucose treated retinas and controls as well as the use of metabotropic receptor antagonists and/or transporter blockers instead of an AMPA/Kainate receptor antagonist (CNQX) in order to isolate any possible discrepancies in oscillatory potentials. As stated previously, ERG recordings from diabetic patients show changes in oscillatory potentials as a marker for the progression of diabetic retinopathy. By studying the impact of hyperglycemia on these wave forms, we could determine if the

## REFERENCES

- Alvarez, Y., M. L. Cederlund, et al. (2007). "Genetic determinants of hyaloid and retinal vasculature in zebrafish." BMC Dev Biol **7**: 114.
- Alvarez, Y., K. Chen, et al. (2010). "Predominant cone photoreceptor dysfunction in a hyperglycaemic model of non-proliferative diabetic retinopathy." Disease Models & Mechanisms **3**(3-4): 236-245.
- Bolzán, A. D. and M. S. Bianchi (2002). "Genotoxicity of Streptozotocin." Mutation Research/Reviews in Mutation Research **512**(2–3): 121-134.
- Caldwell, R. B., A.E.B El-Remessy, R.W. Caldwell. (2008). Oxidative Stress in Diabetic Retinopathy. Diabetic Retinopathy. E. J. Duh. Boston, Humana Press: 3-135.
- Cao, R., L. D. E. Jensen, et al. (2008). "Hypoxia-Induced Retinal Angiogenesis in Zebrafish as a Model to Study Retinopathy." PLoS ONE **3**(7): 1-9.
- Connaughton, V. P. and R. Nelson (2000). "Axonal stratification patterns and glutamate-gated conductance mechanisms in zebrafish retinal bipolar cells." The Journal of Physiology **524**(1): 135-146.
- Danis, R. P. a. M. D. D. (2008). Proliferative Diabetic Retinopathy. Diabetic Retinopathy. E. J. Duh. Boston, Humana Press: 3-135.
- Deshpande, A. D., M. Harris-Hayes, et al. (2008). "Epidemiology of diabetes and diabetes-related complications." Phys Ther **88**(11): 1254-1264.
- Dooley, K. and L. I. Zon (2000). "Zebrafish: a model system for the study of human disease." Current Opinion in Genetics & Development **10**(3): 252-256.

- Dowling, J. E. (1987). The retina : an approachable part of the brain. Cambridge, Mass., Belknap Press of Harvard University Press.
- Ewing, F. M., I. J. Deary, et al. (1998). "Seeing beyond retinopathy in diabetes: electrophysiological and psychophysical abnormalities and alterations in vision." Endocr Rev **19**(4): 462-476.
- Funatsu, H., T. Yamashita, et al. (2006). "Vitreous fluid biomarkers." Adv Clin Chem **42**: 111-166.
- Gleeson, M. C., Victoria. Arneson, Lynn (2006). "Induction of hyperglycemia in zebrafish (*Danio rerio*) leads to morphological changes in the retina." Acta Diabetol **44**: 157-163.
- Lorenzi, M. a. P. O. (2008). The Polyol Pathway and Diabetic Retinopathy. Diabetic Retinopathy. E. J. Duh. Boston, Humana Press: 159-185.
- Menke, A. L., J. M. Spitsbergen, et al. (2011). "Normal anatomy and histology of the adult zebrafish." Toxicol Pathol **39**(5): 759-775
- Meyerle, C. B., E. Chew, F. L Ferris III (2008). Nonproliferative Diabetic Retinopathy. Diabetic Retinopathy. E. J. Duh. Boston, Humana Press: 3-135.
- Moss, J. B., P. Koustubhan, et al. (2009). "Regeneration of the pancreas in adult zebrafish." Diabetes **58**(8): 1844-1851.
- Nestler, E. J., S. E. Hyman, et al. (2009). Molecular neuropharmacology : a foundation for clinical neuroscience. New York, McGraw-Hill Medical.
- Niemeyer G. Das Elektroretinogramm: Nutzlich and Nicht Kompliziert. *Ophta Schweizer. Fachzeitschrift augenarztliche Medizin*. 2004 (5): 7-13, 2004

- Olsen, A. S., M. P. Sarras, Jr., et al. (2010). "Limb regeneration is impaired in an adult zebrafish model of diabetes mellitus." Wound Repair Regen **18**(5): 532-542.
- Papakostopoulos, J.C.Dean Hart, R.J.M. Corral, B. Harney (1996). "The scotopic electroretinogram to blue flashes and pattern reversal visual evoked potentials in insulin dependent diabetes." International Journal of Psychophysiology, **21**(1): 33-43
- Pfister, F., Y. Feng, and HP Hammes (2008). Pericyte Loss in the Diabetic Retina. Diabetic Retinopathy. E. J. Duh. Boston, Humana Press: 245-263.
- Phipps, J. A., P. Yee, et al. (2006). "Rod photoreceptor dysfunction in diabetes: activation, deactivation, and dark adaptation." Invest Ophthalmol Vis Sci **47**(7): 3187-3194.
- Pisharath, H., J. M. Rhee, et al. (2007). "Targeted ablation of beta cells in the embryonic zebrafish pancreas using E. coli nitroreductase." Mechanisms of Development **124**(3): 218-229.
- Purves, D., G. Augustine, D. Fitzpatrick, W. C. Hall, A.S. Lamantia, J. O. McNamara, L. E. White, Ed. (2008). Neuroscience. Sunderland, Sinauer Associates, Inc.
- Robinson, J., E. A. Schmitt, et al. (1995). "Temporal and spatial patterns of opsin gene expression in zebrafish (Danio rerio)." Vis Neurosci **12**(5): 895-906.
- Sherwood, L., H. Klandorf, et al. (2005). Animal physiology : from genes to organisms. Australia ; Belmont, CA, Thomson/Brooks/Cole.
- Stitt, A. W. (2008). The Role of Advanced Glycation in Diabetic Retinopathy. Diabetic Retinopathy. E. J. Duh. Boston, Humana Press: 187-205.
- Szkudelski, T. (2001). "The mechanism of alloxan and streptozotocin action in B cells of the rat pancreas." Physiol Res **50**(6): 537-546.

Tzekov, R. and G. B. Arden (1999). "The electroretinogram in diabetic retinopathy."

Surv Ophthalmol **44**(1): 53-60.

Yazulla, S. and K. M. Studholme (2001). "Neurochemical anatomy of the zebrafish retina as determined by immunocytochemistry." J Neurocytol **30**(7): 551-592.